JETIR.ORG ISSN: 2349-5162 | ESTD Year : 2014 | Monthly Issue
JOURNAL OF EMERGING TECHNOLOGIES AND INNOVATIVE RESEARCH (JETIR)
An International Scholarly Open Access, Peer-reviewed, Refereed Journal

WATER QUALITY INDEX-BASED ASSESSMENT OF SEASONAL AND SPATIO-TEMPORAL DYNAMICS IN THE BHATSA RIVER, MAHARASHTRA

[1]Agre Pradnyesh, [2] Dr. Barabde Gayatri

[1] Research Student, Department of Environmental Science, The Institute of Science, Mumbai 32, India
Email: pa.raj1509@gmail.com
[2] Professor, HOD, Department of Environmental Science, The Institute of Science, Mumbai 32, India
Email: grbarabde@gmail.com

Abstract: The Bhatsa River originates in Igatpuri, Maharashtra, and converges with the Ulhas and Kalu Rivers. This river is a major source of drinking water for the local population and the Mumbai Metropolitan Region (MMR), and supports rich flora and fauna, but also receives pollutants from agriculture, fishing, dredging, and industry. This study examines the seasonal variations in the physicochemical and biological parameters of the Bhatsa River. Significant seasonal fluctuations were observed in turbidity, dissolved oxygen, nutrients and microbial counts. Bhatsa River water quality was evaluated using a multi-parameter Water Quality Index (WQI) at eight stations(S1-S8) from January 2020 to September 2025 across pre-monsoon, monsoon and post-monsoon seasons, measuring monthly pH, dissolved oxygen, biochemical oxygen demand (BOD), chemical oxygen demand (COD), nitrate, fecal coliform(MPN), through Laboratory analysis in accordance with corresponding IS standards and NSFWQI. Mean WQI showed Excellent conditions at upstream S1 (88.43), Good quality at midstream stations S2–S7 (≈78–83), and Poor quality at downstream S8 (56.16), where 69.6% of samples were Very Poor with markedly elevated BOD, COD, and fecal coliform. Kruskal–Wallis tests indicated highly significant spatial differences for all parameters and WQI ($p < 0.001$), while temporal analyses revealed significant WQI decline at S2 and S3, additional concern at S7, increasing pH and nitrate at all stations and sharply rising fecal coliform at S8. Seasonally, WQI was highest in pre- and post-monsoon and lowest during the monsoon, reflecting runoff, dilution, and pollutant loading dynamics. Strong negative correlations of WQI with BOD, COD, and fecal coliform, and positive correlation with dissolved oxygen, highlighted the dominance of organic and microbial pollution, whereas clustering and a pollution severity index delineated three zones: pristine upstream (S1), moderately impacted midstream (S2–S7), and a critical downstream hotspot (S8). Land cover data were obtained from the Esri Sentinel-2 10 m Land Use/Land Cover Time Series, produced by Impact Observatory, Microsoft, and Esri from ESA Sentinel-2 imagery and accessed via the Esri Land Cover Explorer (ArcGIS Living Atlas of the World). Land-cover analysis reveals rapid peri-urban transformation (2017–2024), with built-up area doubling from 3.4% to 7.4% alongside sharp declines in tree cover (21.7% to 14.0%), signalling urgent needs for sustainable planning. The findings confirm a progressive upstream–downstream deterioration in Bhatsa River water quality, with statistically significant inter-station differences and emerging temporal degradation at key midstream sites. These patterns underscore the need for targeted management, including urgent intervention at station S8 and stricter basin-wide control of organic and microbial pollution sources. Seasonal runoff and anthropogenic inputs are shown to exert a strong influence on water quality dynamics, further complicating the river's ecological resilience. Importantly, the integration of hydrological modelling with water quality assessment provides a comprehensive framework to disentangle natural variability from human-induced pressures, offering critical insights into the drivers of river health and guiding sustainable management strategies.

Keywords: **Bhatsa River, Water Quality Index, seasonal variation, watershed analysis, LULC**

1 INTRODUCTION

Rivers are indispensable freshwater resources supporting domestic, agricultural, industrial, and ecological needs, yet rapid urbanization, population growth, and land use changes have contributed to declining water quality worldwide. Seasonal fluctuations, particularly in monsoon-influenced regions such as Maharashtra, cause substantial variation in physico-chemical and biological parameters.[1][2]. Understanding how watershed characteristics and LULC dynamics influence seasonal water quality is crucial for sustainable river basin management, and GIS and remote sensing have emerged as powerful tools for watershed analysis, hydrological modelling, and environmental monitoring[3]

Globally, rivers have become repositories for treated and untreated sewage and industrial effluents, leading to serious deterioration of water quality. Over the past two decades, contamination of inland waters has increased dramatically due to pollutants from point

and non-point sources such as industrial effluents, mining, agricultural waste, and domestic sewage. Rapid industrialization and population growth have exacerbated this problem, introducing toxic chemicals that alter aquatic species diversity and abundance, with developing countries facing particular challenges from large-scale discharge of untreated industrial and domestic waste. Historically, rivers have served as outlets for urban sewage and industrial effluents, with both point and non-point sources degrading river health [4]. Freshwater contamination has increased due to heavy metals and organic pollutants ([5]; [6]; [7], [8], [9]), while industrial pollutants, often toxic and persistent, harm rivers by altering species diversity and abundance.[1], [7], [10], [11] Many developing regions face mounting challenges from untreated effluents as chemical use surges ([12] [13]).

Water resource management has gained prominent international attention due to mounting pressures from rapid economic development, expanding populations, climate change impacts, and public health requirements. [14] The United Nations 2030 Agenda's Sustainable Development Goal 6 (SDG6) focuses exclusively on water challenges, targeting universal access to safe water and sanitation while promoting integrated water resource management strategies. [15]. Systematic water quality assessment provides essential data for effective watershed governance, regulatory compliance verification, and ecosystem protection. [16], [17] Although comprehensive global water quality datasets remain limited—particularly from developing regions—monitoring efforts have intensified through targeted research initiatives. [18]

Water quality evaluation examines physical, chemical, and biological characteristics to determine suitability for specific uses, establishing baseline conditions against which pollution impacts can be measured. [19]. This quantitative framework supports critical functions, including: Evidence-based water resource decision-making [20], establishing an early detection system (including chemical and microbial contamination, eutrophication, emerging contaminants, issues related to climate change, among others), Verification of regulatory compliance, Protection of designated water uses (potable supply, recreation, aquatic life), Analysis of temporal pollution trends[21] and in the Assessment of ecological impacts on aquatic ecosystems [22].

Seasonal fluctuations strongly influence pollutant concentrations. Monsoon runoff introduces high organic loads, sediments, turbidity, nutrient loading, and microbial contamination [23][24], while dilution improves dissolved oxygen but elevates suspended solids. In drier seasons, pollutants become concentrated. Resource availability (organic carbon, nitrogen, phosphorus) and food-web dynamics shape freshwater bacterial communities [25]; [26]; [27][28], while environmental factors such as water-column stability, stratification, and temperature drive seasonal shifts ([29], [30]). Monitoring physico-chemical parameters such as salinity, temperature, and pH provides insight into microbial community dynamics and their response to changing conditions ([31]). Life originated in aquatic environments billions of years ago, and most major taxonomic groups still inhabit water bodies ([32], [33]), underscoring the importance of maintaining river health. Thus, the objective of this study is to monitor seasonal water quality in the Bhatsa River using physico-chemical and microbiological indicators.

Watershed characteristics influence hydrological responses, affecting pollutant transport and sedimentation [34] LULC changes, particularly urbanization and agriculture, are major contributors to water degradation [35]. GIS-integrated water quality studies have shown strong correlations between land use patterns and water quality indices in Indian river basins. [36], [37], [38], [39]

The Bhatsa River is a major tributary of the Ulhas River system in Maharashtra, serving as an important water resource for drinking water supply, irrigation, and industrial use. Monitoring of water quality is essential for: Assessing compliance with national water quality standards identifying pollution sources and mitigation strategies supporting environmental impact assessments and regulatory decisions, and informing water resource management and planning.[34], [40], [41], [42]

The Water Quality Index (WQI) is a composite indicator that combines multiple water quality parameters into a single numerical score, facilitating rapid communication of water quality status to policymakers and stakeholders [6]. WQI values span 0 to 100; a higher WQI indicates fewer pollutants and healthier aquatic conditions, while lower values signal degraded water quality.

The primary objectives of this analysis are to: Evaluate temporal and spatial patterns in WQI across monitoring stations, identify statistically significant trends in water quality over the 2020–2025 period, assess seasonal variations and their implications, compare water quality between upstream and downstream locations, Provide evidence-based recommendations for water quality management.

2 Materials and Methods

2.1 Study Area:

The Bhatsa River is an important tributary of the Ulhas River, located in Thane district, Maharashtra. It originates in the Western Ghats near Kasara (Igatpuri region) and flows through Shahapur, covering approximately 80 km in length before joining the Ulhas system (Maharashtra Pollution Control Board). The watershed extends from Shahapur to Ambivli, encompassing several villages including Bhatsa, Sapgaon, Vasind, Bhatsei, Koshimbi, Khadavli, Shere, Pise, Vasundri, Vaveghar, and Nadgaon etc. At Ambivli, the Bhatsa River merges with the Kalu River (flowing through Murbad district). From Kalyan onward, the combined stream flows toward Diva and Mumbra, eventually emptying into the Thane Creek. Overall, the river travels about 80 km from Bhatsa village to its confluence with the Ulhas River. Importantly, as per Census 2011, Rural areas. Thus, around 22.5% (70,710) of the total population (314,103) of Shahapur Taluka lives in Urban areas, while 77.5% (243,393) lives in Rural areas. People depend on the Bhatsa River for drinking water and other purposes. The region experiences three major seasons: pre-monsoon (dry), monsoon (wet) and post-monsoon (transition). Sampling locations were selected based on land use variability, accessibility and anthropogenic influences.

The Bhatsa River, an important tributary of the Ulhas River, is located in Thane district, Maharashtra. It originates in the Western Ghats near Kasara, flows through Shahapur (encompassing villages such as Bhatsa, Sapgaon, Vasind, Bhatsei, Koshimbi, Khadavli, Shere, Pise, Vasundri, Vaveghar, and Nadgaon), and covers approximately 80 km before merging with the Kalu River at Ambivli. From Kalyan onward joining the Ulhas system, the combined stream flows toward Diva and Mumbra, eventually emptying into Thane Creek. According to the 2011 Census, Shahapur Taluka is predominantly rural, with 77.5% of its population in rural areas and 22.5% in urban areas. Local communities depend on the Bhatsa River for drinking water and other purposes. The region

experiences three major seasons: pre-monsoon, monsoon, and post-monsoon. Sampling locations were selected based on land use variability, accessibility, and anthropogenic influences

Taking into account the water requirements of the Mumbai Municipal Corporation, a High-Powered Committee was established in 1961 to ensure adequate water supply. The Bhatsa Project was sanctioned by the Government of Maharashtra in 1964. Under this, a Bhatsa dam was constructed in two phases at Sajivali village, Shahapur taluka, at the confluence of the Bhatsa and Chorana rivers.[43] The Bhatsa Project is a major multipurpose project located in Shahapur taluka of Thane district. Its objectives include providing irrigation benefits to 9,190 hectares of land in Shahapur and Bhiwandi talukas, generating 15 MW of electricity and supplying drinking water to the Brihanmumbai Municipal Corporation as well as to the growing population of Thane district, Bhiwandi Nizampur Municipal Corporation, Industrial establishments, Gram Panchayats – 38, Shahapur Nagar Panchayat, and other institutions.

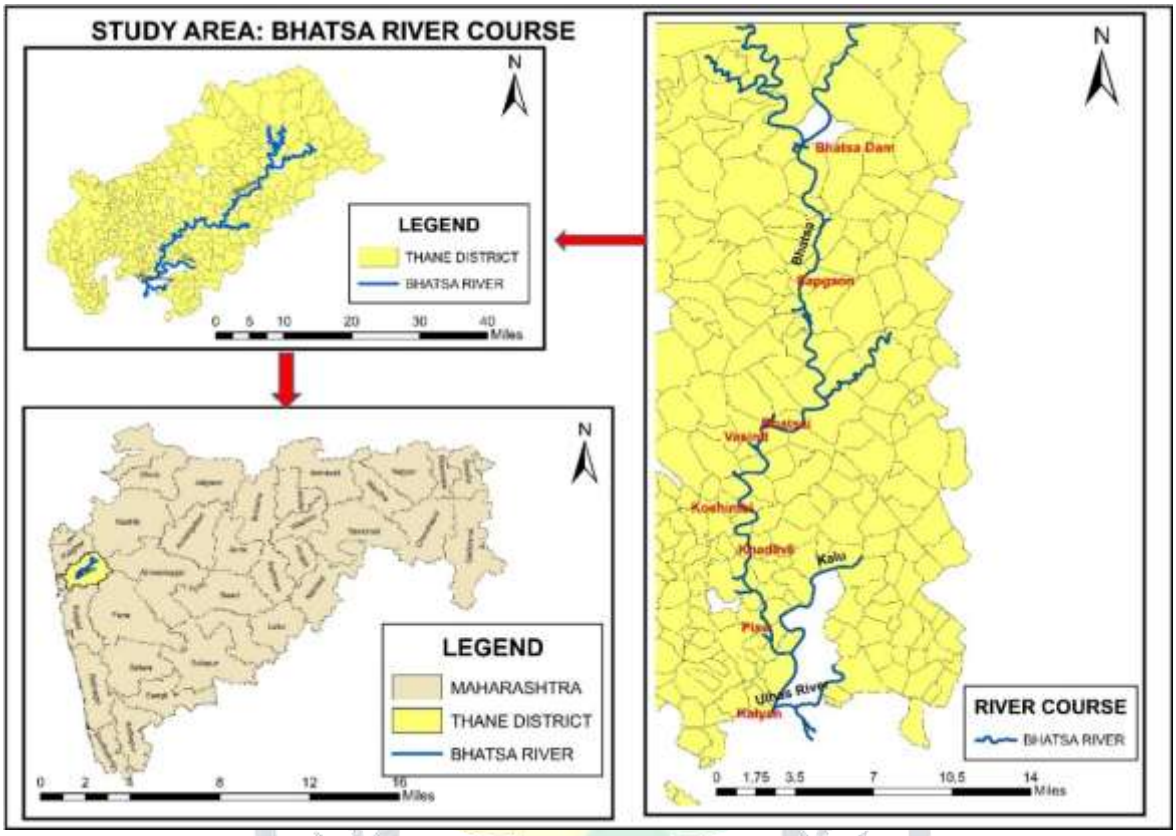

Figure 1: Bhatsa River course

2.2 Sampling Locations:

The study included eight sampling sites along the Bhatsa River (Table 1). These locations were chosen to represent upstream (near the dam), midstream (agricultural and industrial areas) and downstream (urban convergence) environments. The **Table 1Table 1** lists coordinates and potential pollution sources at each site.

Table 1 Sampling locations.

Sr. No.	Location	Coordinates (N, E)	Possible Polluting Sources
S1	Bhatsa Dam	19.5131°, 73.4174°	Surface runoff
S2	Sapgaon	19.4481°, 73.3590°	Industries; Pilgrimage site, Local human activities
S3	Bhatsei	19.3958°, 73.2768°	Agricultural runoff, Cattle washing
S4	Vasind	19.4099°, 73.2659°	Industries; Recreation area
S5	Koshimbi	19.3816°, 73.2221°	Agricultural runoff, Cattle washing
S6	Khadavli	19.3561°, 73.2179°	Sewage discharge; Recreation and pilgrimage area
S7	Pise	19.3173°, 73.1803°	Recreation area; Dredging activity
S8	Kalyan	19.2463°, 73.1308°	Confluence with Ulhas & Kalu Rivers; Ship repair/maintenance; Industries; Open dumping ground; Recreation/pilgrimage site

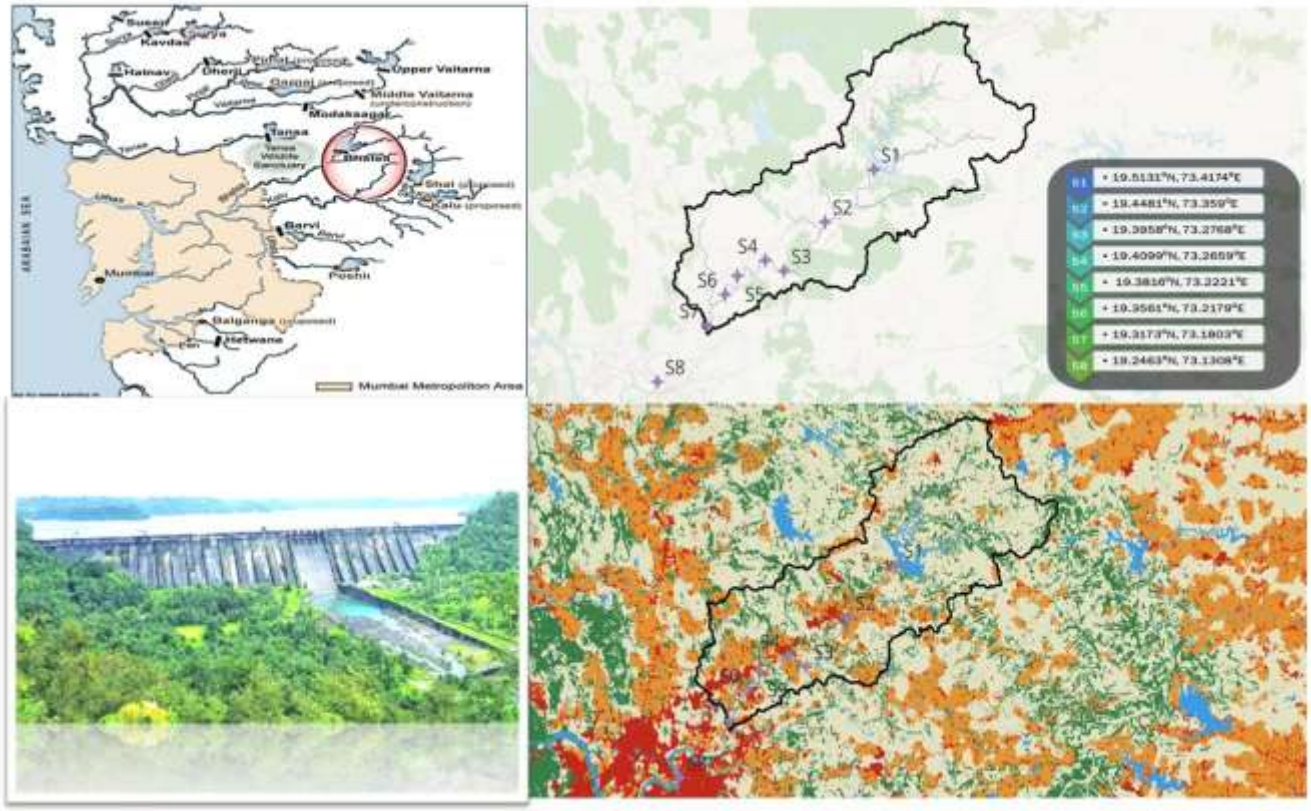

Figure 2: Overview of study area and sampling locations

2.3 Water Sampling and Laboratory Analysis

Water samples were collected from selected sites in the pre-monsoon, monsoon and post-monsoon seasons. Water samples were collected monthly over a period (January 2020-September 2025) at the 8 locations shown in Table 1. Sampling was done in daylight, following the river's flow direction, and water was sampled *against the flow* to ensure representativeness. For microbiological analysis, sterile 100 mL wide-mouthed bottles were used; for physico-chemical analysis, 5-L polyethylene cans were employed. Each sample bottle was labelled with date, time and location. Collected samples were transported in cool (Icebox) and dark conditions to the laboratory and analysed within 24 hours of collection. Parameters analysed in perspective of WQI included pH, DO, BOD, COD, nitrates and MPN, determined following standard procedures described by APHA (2017) and corresponding Indian Standard methods (IS 3025 Parts 34, 38, 44 and IS 1622:1981) for water and wastewater analysis.[44] .

2.3.1 Physico-Chemical Analysis

Physico-chemical parameters were measured using standard methods as per APHA 2017 [44]. Water temperature was recorded on-site with a standard thermometer (0–100 °C). pH was first checked using broad-range pH paper and later confirmed with a calibrated pH meter. Dissolved Oxygen (DO) was fixed on-site using Winkler's reagent. In the laboratory, parameters such as Chemical Oxygen Demand (COD), Biological Oxygen Demand (BOD), Nitrates and MPN were measured according to APHA standard protocols. Each measurement was replicated, and laboratory blanks and standards were used for quality control. Results are reported as average values from replicate analyses.

2.3.2 Microbiological Analysis (MPN)

Fecal coliform counts were determined by the Most Probable Number (MPN) technique using multiple-tube fermentation. Presumptive Test: Aliquots of water samples were inoculated into MacConkey broth tubes containing inverted Durham tubes. Tubes were incubated at 37 °C for 24 hrs. Positive indication was confirmed by lactose fermentation with gas production. The number of positive tubes was recorded, and the MPN per 100 mL was estimated using standard probability tables. All media and reagents were obtained from HiMedia Laboratories, Mumbai. Sterility controls were run with each batch of tests.

2.4 Water Quality Index (WQI)

The Water Quality Index (WQI) provides a standardized method for aggregating multiple water quality parameters into a single comprehensive metric, facilitating spatial comparison and temporal trend analysis across river reaches [Ott, 1978]. In India, the **CPCB-modified National Sanitation Foundation Water Quality Index (NSFWQI)** has been adopted as the national standard for surface water quality assessment, with adjusted parameter weights optimized for Indian river conditions. [[41], [42]; [45]

The CPCB-modified NSFWQI was calculated using the arithmetic aggregation model. The Weighted Quality Index (WQI) is calculated using the following equations:

$$WQI = \sum_{i}^{n} W_i Q_i$$

$$I = \sum_{i=1}^{n} I_i W_i$$

Here

$\sum_{i=1}^{n} W_i = 1$

$(I_i) =$ Sub − index of individual parameter

$(W_i) =$ Weight factor

$(Q_i) =$ Value of rating parameter i

$(n) =$ Number of sub − indices

2.4.1 Data Processing Protocol

Monthly composite samples (n = 552; 8 stations, January 2020–September 2025) were analyzed following the CPCB-modified NSFWQI protocol. For each sample, pH, dissolved oxygen (DO), biochemical oxygen demand (BOD), chemical oxygen demand (COD), nitrate, and fecal coliform (FC, reported as MPN/100 mL) were measured and converted into individual sub-indices ranging from 0 to 100 using standard equations, with lower sub-indices reflecting poorer quality for each parameter. These sub-indices were then aggregated into a single Water Quality Index (WQI) using CPCB-prescribed weights, as illustrated in Figure 3.

NSFWQI classification scheme applied in this study: WQI values of 63–100 are classified as Good to Excellent (non-polluted), 50–63 as Medium to Good (non-polluted), 38–50 as Bad (polluted), and ≤38 as Bad to Very Bad (heavily polluted), providing a consistent framework for interpreting spatial and temporal water-quality patterns along the river.

Figure 3 WQI calculation

2.5 Statistical Methods

2.5.1 Descriptive Statistics

For each sampling site, descriptive statistics were computed, including mean, median, minimum, maximum, standard deviation (SD), quartiles (Q1, Q3), interquartile range (IQR), coefficient of variation (CV%), skewness and kurtosis. These measures provided an overview of central tendency, dispersion and distributional characteristics of the water quality index (WQI).

2.5.2 Comparative Analysis

Parametric tests: One-way ANOVA was applied to assess significant differences in mean WQI among sites. Pearson correlation and linear regression were used to evaluate relationships between physicochemical parameters and WQI.

Non-parametric tests: The Kruskal–Wallis H-test was employed to validate findings without assuming normality. Spearman's rank correlation was used to examine monotonic associations. [46]

Post-hoc tests: Pairwise comparisons were conducted using Tukey's HSD test for ANOVA results, and the Mann–Whitney U test with Bonferroni correction (adjusted $\alpha = 0.0018$) for non-parametric outcomes.

2.5.3 Temporal Trend Analysis

To detect long-term changes, linear regression was performed on WQI values against time (converted to a continuous year scale). The Mann–Kendall test was additionally applied to identify monotonic trends. Statistical significance was evaluated at a threshold of $p < 0.05$.

2.5.4 Multivariate Analysis

K-means clustering (k = 3) was conducted to classify sites based on similarity in water quality profiles. Correlation analysis among clusters was performed to explore interdependencies between parameters.

2.5.5 Seasonal Analysis

Quarterly aggregation of WQI statistics was carried out to capture seasonal variability. Differences between monsoon and non-monsoon periods were specifically assessed to highlight hydrological influences on water quality.

2.6 Land Use/Land Cover Classification

Land-cover dynamics were quantified using the Esri Sentinel-2 Land Cover Time Series, which provides annual global maps from 2017 onwards at 10 m spatial resolution. The maps are generated by a deep learning classification model developed by Impact Observatory, Microsoft, and Esri, trained on billions of human-labelled Sentinel-2 pixels and producing nine land-use/land-cover (LULC) classes: Water, Trees, Flooded Vegetation, Crops, Built Area, Bare Ground, Snow/Ice, Clouds, and Rangeland.[47], [48], [49], [50], [51], [52], [53], [54], [55], [56], [57], [58]

The analysis focused on the area defined in the Land Cover Explorer centred near 19.42°N, 73.30°E, corresponding to the rapidly urbanizing fringe east of Mumbai, and extracted class-wise proportional cover for each year from 2017 to 2024. Annual class proportions were compiled into a time series to assess trajectories of urban expansion, agricultural transition, and vegetation change at the landscape scale.[59]

3 Results and Discussion

The study encompasses a comprehensive dataset spanning January 2020 to September 2025 (69 months) across eight monitoring stations (S1–S8), with parameters including pH, dissolved oxygen (DO), biochemical oxygen demand (BOD), chemical oxygen demand (COD), nitrate, fecal coliform (FC), and water quality index (WQI), yielding 552 total observations (69 per station).

Seasonal stratification was applied as follows: pre-monsoon (March–May; 18 records per station), monsoon (June–September; 24 records per station), and post-monsoon (October–February; 27 records per station).

3.1 Descriptive statistics by location

Descriptive statistics were computed both overall (Table 2)and for each sampling site(Table 3), encompassing measures such as mean, median, minimum, maximum, standard deviation (SD), quartiles (Q1, Q3), interquartile range (IQR), coefficient of variation (CV%), skewness, and kurtosis. These statistical indicators provide a comprehensive overview of the central tendency, dispersion, and distributional characteristics of the water quality index (WQI), with the results summarized in (Table 4). S8 shows extremely high variability (CV > 70%) for pollution indicators (BOD, COD, FC, Nitrate), indicating highly unstable and degraded conditions.

Table 2 : Overall Descriptive statistical analysis at the Bhatsa River Basin

Parameter	Count	Mean	Median	SD	CV%	Min	Q25	Q75	Max	Skewness	Kurtosis
pH	552	7.59	7.60	0.32	4.1591	6.40	7.400	7.800	8.80	0.0894	0.2487
DO	552	6.94	7.20	1.00	14.4277	0.80	6.900	7.400	8.00	-3.0044	10.2420
BOD	552	5.34	3.80	5.90	110.5371	0.40	3.200	4.800	50.00	4.3412	21.4865
COD	552	22.07	16.00	27.20	123.2394	4.00	12.000	20.000	168.00	3.5078	12.1444
Nitrate	552	0.64	0.40	1.00	155.8532	0.00	0.300	0.500	11.56	5.7146	41.8305
FC	552	25.02	12.00	57.45	229.6270	0.00	7.000	21.000	900.00	8.8334	109.1006
WQI	552	78.21	80.21	9.82	12.5503	37.38	77.335	83.002	96.22	-1.9591	3.9567

Table 3 : Descriptive Statistics by Sampling Location (S1-S8) (2020-2025)

Station & Parameters	*Mean*	*Median*	*SD*	*Min*	*Max*	*IQR*	*CV*
S1							
BOD	2.406	2.400	0.974	0.400	6.000	1.200	40.501
COD	8.377	8.000	2.855	4.000	16.000	0.000	34.080
DO	7.400	7.400	0.219	6.800	8.000	0.200	2.959
FC	4.478	4.000	3.357	0.000	17.000	4.000	74.967
Nitrate	0.347	0.300	0.140	0.100	0.890	0.100	40.303
pH	7.343	7.300	0.215	7.000	7.900	0.300	2.931
WQI	88.431	88.363	2.870	82.229	96.223	3.796	3.246
S2							
BOD	3.719	3.600	0.964	2.400	7.000	1.000	25.912
COD	13.913	12.000	4.036	8.000	28.000	4.000	29.006
DO	7.170	7.200	0.290	6.300	7.700	0.400	4.040
FC	11.026	11.000	6.254	1.800	34.000	7.000	56.719
Nitrate	0.360	0.300	0.158	0.000	1.100	0.110	43.732
pH	7.712	7.700	0.294	7.200	8.600	0.400	3.810
WQI	81.028	80.785	2.863	74.594	88.069	3.270	3.533
S3							
BOD	3.754	3.600	0.952	2.400	7.000	0.800	25.375
COD	13.797	12.000	3.913	8.000	24.000	4.000	28.361
DO	7.043	7.100	0.337	5.900	7.500	0.300	4.787
FC	12.928	11.000	6.835	5.000	50.000	9.000	52.871

Station & Parameters	*Mean*	*Median*	*SD*	*Min*	*Max*	*IQR*	*CV*
Nitrate	0.387	0.370	0.137	0.000	0.800	0.160	35.465
pH	7.670	7.700	0.318	6.900	8.800	0.300	4.143
WQI	80.246	80.313	2.449	74.254	84.956	3.394	3.052
S4							
BOD	4.155	3.800	1.268	2.400	10.000	1.200	30.525
COD	16.377	16.000	4.106	8.000	28.000	8.000	25.070
DO	7.074	7.100	0.281	6.200	7.600	0.300	3.966
FC	15.884	14.000	7.783	4.000	40.000	13.000	48.999
Nitrate	0.379	0.390	0.120	0.100	0.900	0.110	31.652
pH	7.706	7.700	0.258	6.800	8.300	0.300	3.345
WQI	78.730	78.552	2.686	71.515	84.785	2.975	3.411
S5							
BOD	4.075	4.000	1.045	2.600	8.000	1.200	25.654
COD	15.116	16.000	4.086	8.000	24.000	4.000	27.029
DO	7.245	7.300	0.255	6.400	7.700	0.300	3.523
FC	15.613	14.000	8.627	4.500	60.000	12.000	55.253
Nitrate	0.428	0.400	0.143	0.200	1.000	0.200	33.331
pH	7.581	7.600	0.304	6.400	8.200	0.400	4.010
WQI	80.198	80.066	2.359	75.378	85.603	3.543	2.942
S6							
BOD	4.857	4.600	1.231	2.800	8.000	1.800	25.346
COD	18.522	20.000	4.636	12.000	32.000	4.000	25.028
DO	7.487	7.600	0.242	6.800	7.900	0.200	3.231
FC	18.475	17.000	12.892	5.000	90.000	11.000	69.779
Nitrate	0.423	0.400	0.133	0.100	0.800	0.200	31.374
pH	7.768	7.800	0.269	7.200	8.400	0.400	3.466
WQI	78.146	78.216	2.830	69.985	83.494	3.936	3.621
S7							
BOD	3.501	3.400	0.865	1.400	6.400	1.000	24.697
COD	12.406	12.000	4.052	4.000	28.000	8.000	32.665
DO	7.297	7.300	0.271	6.100	7.800	0.300	3.716
FC	10.229	8.000	6.024	2.000	33.000	8.000	58.891
Nitrate	0.388	0.390	0.122	0.100	0.790	0.190	31.399
pH	7.574	7.600	0.281	6.800	8.300	0.400	3.704
WQI	82.745	82.041	2.545	78.343	88.308	3.951	3.075
S8							
BOD	16.268	12.000	11.529	3.800	50.000	15.000	70.868
COD	78.072	72.000	46.748	8.000	168.000	84.000	59.878
DO	4.774	4.900	1.417	0.800	7.200	1.700	29.684
FC	111.522	70.000	132.297	17.000	900.000	90.000	118.629
Nitrate	2.407	1.800	2.074	0.300	11.560	1.800	86.162
pH	7.378	7.300	0.299	6.800	8.300	0.400	4.052
WQI	56.158	55.271	9.703	37.378	80.097	13.595	17.278

Table 4: Summary Descriptive Statistics by Location and Parameters (Mean ± Sd; Range)

Station	pH	DO (mg/L)	BOD (mg/L)	COD (mg/L)	Nitrate (mg/L)	FC (MPN/100mL)	WQI
S1	7.34±0.22 (7.0-7.9)	7.40±0.22 (6.8-8.0)	2.41±0.97 (0.4-6.0)	8.38±2.85 (4.0-16.0)	0.35±0.14 (0.1-0.9)	4.48±3.36 (0-17)	88.43±2.87
S2	7.71±0.29 (7.2-8.6)	7.17±0.29 (6.3-7.7)	3.72±0.96 (2.4-7.0)	13.91±4.04 (8-28)	0.36±0.16 (0-1.1)	11.03±6.25 (1.8-34)	81.03±2.86
S3	7.67±0.32 (6.9-8.8)	7.04±0.34 (5.9-7.5)	3.75±0.95 (2.4-7.0)	13.80±3.91 (8-24)	0.39±0.14 (0-0.8)	12.93±6.83 (5-50)	80.25±2.45
S4	7.71±0.26 (6.8-8.3)	7.07±0.28 (6.2-7.6)	4.16±1.27 (2.4-10)	16.38±4.11 (8-28)	0.38±0.12 (0.1-0.9)	15.88±7.78 (4-40)	78.73±2.69
S5	7.58±0.30 (6.4-8.2)	7.24±0.26 (6.4-7.7)	4.08±1.05 (2.6-8.0)	15.12±4.09 (8-24)	0.43±0.14 (0.2-1.0)	15.61±8.63 (4.5-60)	80.20±2.36
S6	7.77±0.27 (7.2-8.4)	7.49±0.24 (6.8-7.9)	4.86±1.23 (2.8-8.0)	18.52±4.64 (12-32)	0.42±0.13 (0.1-0.8)	18.48±12.89 (5-90)	78.15±2.83
S7	7.57±0.28 (6.8-8.3)	7.30±0.27 (6.1-7.8)	3.50±0.86 (1.4-6.4)	12.41±4.05 (4-28)	0.39±0.12 (0.1-0.8)	10.23±6.02 (2-33)	82.75±2.55
S8	7.38±0.30 (6.8-8.3)	4.77±1.42 (0.8-7.2)	16.27±11.53 (3.8-50)	78.07±46.75 (8-168)	2.41±2.07 (0.3-11.6)	111.52±132.30 (17-900)	56.16±9.70

3.1.1 pH (Acidity/Alkalinity)

The river exhibited predominantly alkaline conditions across all eight monitoring stations, with pH values ranging from 6.4 to 8.8 (mean ± SD: 7.59 ± 0.32; median [IQR]: 7.60 [7.40–7.80]), characteristic of carbonate-buffered freshwater systems.

Reference site S1 maintained stable neutral-alkaline conditions (7.34 ± 0.22, CV = 2.93%), while intermediate sites showed progressively elevated alkalinity, peaking at S6 (7.77 ± 0.27, CV = 3.47%; maximum 8.4). Notably, 75% of measurements across all sites exceeded pH 7.4, with S3 recording the highest value (8.8), indicating strong alkalinity buffering rather than neutral conditions. Downstream site S8 exhibited slightly depressed pH (7.38 ± 0.30, CV = 4.05%) relative to intermediate sites despite severe organic loading, suggesting anaerobic acid production counteracting upstream alkalinity. While within tolerance limits for most aquatic biota (pH 6.5–8.5), the consistently alkaline regime (>7.4 IQR) may favour alkaliphilic species while limiting acid-tolerant taxa.

3.1.2 Dissolved Oxygen (DO)

Dissolved oxygen concentrations spanned 0.8–8.0 mg/L (mean ± SD: 6.94 ± 1.00; median [IQR]: 7.20 [6.90–7.40]), with upstream site S1 showing optimal levels (7.40 ± 0.22; CV = 2.96%) indicative of efficient reaeration and minimal organic demand. Intermediate sites S2–S7 maintained adequate oxygenation (7.04–7.49 mg/L; CV: 3.23–4.79%), supporting most aquatic biota, though S3 exhibited the widest fluctuations (range: 5.9–7.5 mg/L). Critically, downstream site S8 showed severe depletion (4.77 ± 1.42 mg/L; median: 4.90 [4.10–5.80]; CV = 29.68%) with hypoxic events (min: 0.8 mg/L), indicating anaerobic conditions and ecological stress from excessive organic loading. falling below MPCB Class II standards (≥4 mg/L) for fisheries during hypoxic events (min: 0.8 mg/L).

Spatially, S6 consistently exhibited higher DO, attributable to its geomorphology and flow dynamics that enhanced aeration, while S4 and S7 showed lower DO, likely due to slower currents and deeper pools that reduce aeration. The low DO during late monsoon (August–September) suggests elevated organic and inorganic loads, which intensify oxygen consumption and compromise aquatic health. Overall, DO levels increased from August to December, consistent with the inverse relationship between water temperature and oxygen solubility; colder winter waters hold more oxygen (Tiwari et al., 2014). Lowered DO at S8 is indicative of heavy organic pollution and intense microbial oxygen demand. Overall Mean: 6.94 ± 1.00 mg/L DO is generally not a limiting factor except at severely contaminated site S8. This suggests active organic decomposition.

3.1.3 Chemical Oxygen Demand (COD)

COD exhibited the broadest range (4.0–168.0 mg/L; mean ± SD: 22.07 ± 27.20; median [IQR]: 16.00 [12.00–20.00]), highlighting refractory organic accumulation. Site S1 showed baseline levels (8.38 ± 2.85 mg/L; median: 8.00) typical of natural humic loading, with consistent elevation at Intermediate sites S2–S7 (12.41–18.52 mg/L; CV: 25.03–32.66%) demonstrated progressive accumulation, peaking at S6 (median: 20.00). Site S8 demonstrated catastrophic contamination (78.07 ± 46.75 mg/L; median: 72.00 [36.00–120.00]; CV = 59.88%; max: 168.0 mg/L), indicating persistent industrial or complex organic pollutant ingress affecting self-purification capacity, representing an elevation over reference conditions and exceeding MPCB Class II limits (250 mg/L) during episodic events (max: 168 mg/L).

S2& S4 are in proximity to industries (e.g., Liberty Oil Mills, Jindal Steel, SL Packaging, Khanna Pipes, Nexus Steel, plastics and other manufacturing units, etc.), which discharge effluents that contribute to elevating COD. S8 consistently high COD may be due to the confluence of the Bhatsa and already-polluted Ulhas and Kalu rivers that contaminated with Industrial Effluent from MIDCs in their catchment.[9] Retibunder operations ship-repair activities contribute significant organic pollutants, e.g., oil & grease. Moreover, a large open dumping ground & Sewage treatment plant in proximity contributes as leachate and outlet discharges that pours High organic load into the river. These sources combined explain the markedly elevated COD at S8 throughout the study.

3.1.4 Biochemical Oxygen Demand (BOD)

BOD levels ranged from 0.4–50.0 mg/L (mean ± SD: 5.34 ± 5.91; median [IQR]: 3.80 [3.20–4.80]), reflecting a pronounced pollution gradient. Reference site S1 maintained clean conditions (2.41 ± 0.97 mg/L; median: 2.40), while intermediate sites S2–S7 showed moderate elevation (3.50–4.86 mg/L; CV: 24.70–40.51%), crossing into acceptable-to-moderately polluted ranges underscores significant organic pollution due to domestic sewage, agricultural runoff and fertilizer residues and at some rural sites,

likely from human and animal waste, given the river's use for washing and sanitation. Downstream site S8 exhibited severe organic pollution (16.27 ± 11.53 mg/L; median: 12.00 [8.00–23.00]; CV = 70.87%; max: 50.0 mg/L), confirming chronic wastewater influence with extreme episodic contamination events.

According to common water quality classifications, BOD < 3 mg/L is "good quality" (Class 1, suitable for drinking and fisheries), 3–<6 mg/L is "fair quality" (Class 2, needs some treatment), 6–12 mg/L is "poor quality" (Class 3) and ≥12 mg/L is "bad quality" (Class 4, grossly polluted) Biochemical oxygen demand (BOD) values at stations S1–S7 remained within the acceptable limits for both propagation of wildlife/fisheries (≤3 mg/L) and organized outdoor bathing (≤5 mg/L), indicating full compliance with designated best use criteria. In contrast, station S8 exhibited BOD levels that consistently exceeded these thresholds, classifying it as severely non-compliant with the relevant water quality standards for both uses.

3.1.5 Nitrate

Nitrate concentrations ranged from 0.0–11.56 mg/L (mean ± SD: 0.64 ± 0.99; median [IQR]: 0.40 [0.30–0.50]), transitioning from oligotrophic upstream to eutrophic downstream conditions. Reference site S1 showed pristine levels (0.35 ± 0.14 mg/L; median: 0.30), with modest enrichment at S2–S7 (0.36–0.43 mg/L; CV: 31.37–43.73%). Site S8 exhibited severe susceptibility to eutrophication (2.41 ± 2.07 mg/L; median: 1.80 [1.10–2.90]; CV = 86.16%; max: 11.56 mg/L), exceeding drinking water guidelines and confirming major nutrient pollution from sewage or agricultural runoff and other nonpoint sources.

3.1.6 Fecal Coliform (MPN)

Fecal coliform (FC) concentrations followed a pronounced spatial pollution gradient, with reference site S1 exhibiting pristine conditions (mean: 4.0 MPN/100mL) typical of undisturbed watersheds. Intermediate sites S2–S7 showed moderate fecal loading (mean: 12–33 MPN/100mL) consistent with rural agricultural and septic system influences. Critically, downstream site S8 demonstrated severe public health risk (mean: 240 MPN/100mL; median: 70 MPN/100mL; IQR: 33–140 MPN/100mL), with maximum values reaching 900 MPN/100mL and 75% of samples exceeding recreational bathing standards (200 MPN/100mL). The FC elevation at S8, coinciding with BOD and COD increases, confirms chronic, untreated sewage discharge as the dominant pollution vector. This integrated sanitary-chemical contamination profile at the terminal reach underscores critical wastewater infrastructure failure requiring immediate regulatory intervention.

MPN counts at all sites suggest significant fecal loading, likely exacerbated by monsoon rains. Heavy rainfall can cause surface runoff and soil erosion that carry animal and human wastes into the river. Additionally, seasonal factors (optimum temperature around 30 °C, neutral pH, high nutrients) during the rainy season created favourable conditions for coliform growth. By winter, with reduced flow and temperature, coliform growth reduces, and counts decline.

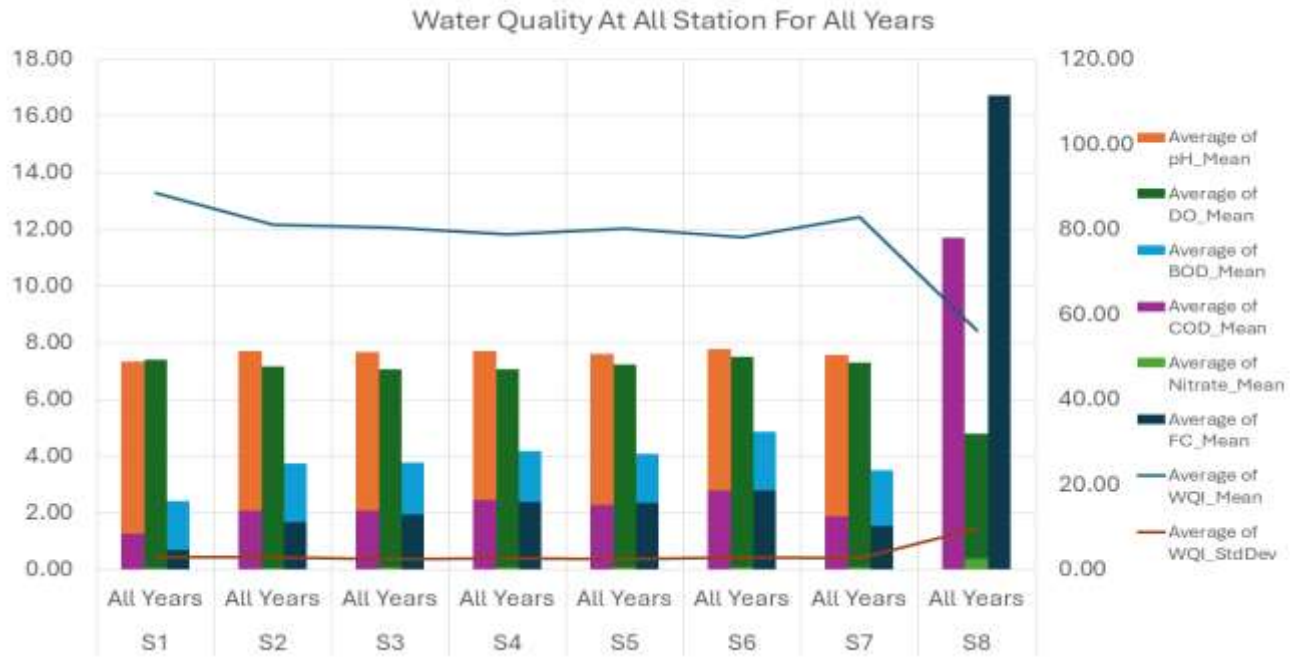

Figure 4 Spatio-Temporal Mean Water Quality and Water Quality Index (WQI)2020-25

3.2 Water Quality Index (WQI)

The CPCB-modified NSFWQI revealed a pronounced spatial degradation gradient across the eight monitoring stations (Table 5 Summary Statistics of NSFWQI by Station (n=69/site), transitioning from excellent upstream conditions to chronically poor downstream quality. Station S1 exhibited pristine conditions (mean WQI: 88.4 ± 3.2, range: 76.6-96.2; "Excellent" Class A), serving as the appropriate reference baseline. Stations S2-S7 maintained good quality (WQI: 78.1-82.7; Class B), suitable for outdoor bathing and propagation of wildlife, while Station S8 demonstrated poor quality (WQI: 56.2 ± 17.3, range: 37.4-88.0; Class C), indicative of significant pollution stress.

Table 5 Summary Statistics of NSFWQI by Station (n=69/site)

Station	Mean WQI ± SD	Median [IQR]	Range	Quality Class	% Time "Good" (>70)
S1	88.4 ± 3.2	89.0 [86.8-91.0]	76.6-96.2	Excellent (A)	100%
S2	81.0 ± 4.8	81.5 [78.0-84.0]	70.2-91.7	Good (B)	97.1%
S3	80.2 ± 5.1	80.5 [77.0-83.5]	68.9-90.1	Good (B)	94.2%
S4	78.7 ± 6.2	79.0 [75.0-82.5]	65.4-88.3	Good (B)	89.9%
S5	80.2 ± 5.4	80.5 [77.5-83.5]	67.8-90.2	Good (B)	92.8%
S6	78.1 ± 7.1	78.5 [74.5-82.0]	62.3-87.2	Good (B)	85.5%
S7	82.7 ± 4.9	83.0 [80.0-85.5]	72.1-92.4	Good (B)	98.6%
S8	56.2 ± 17.3	57.0 [46.7-68.0]	37.4-88.0	Poor (C)	36.2%

3.2.1 Classification Distribution by Station

Water Quality Index (WQI) was interpreted using standard Indian classification thresholds, wherein WQI ≥ 90 denotes Excellent water quality, 80 ≤ WQI < 90 indicates Good quality, 70 ≤ WQI < 80 represents Medium quality, 60 ≤ WQI < 70 corresponds to Poor quality, and WQI < 60 is classified as Very Poor. Overall, the river assessment indicates spatial heterogeneity in water quality: Station S1 alone attains an 'Excellent' status, while the majority of sites (62.5%; S2–S7) consistently exhibit 'Good' quality in more than half of the observations. In contrast, Station S8 is characterized by a predominance of 'Very Poor' quality (69.6%), reflecting severe contamination pressures.

Table 6 WQI Classification & Temporal Distribution

Station	Mean WQI	Status	Trend (per mo.)	Significant	Excellent	Good	Medium	Poor	Very Poor
S1	88.43065	Excellent	-0.03287	No	29.0% (20)	71.0% (49)	0% (0)	0% (0)	0% (0)
S2	81.02822	Good	-0.04267	Yes	0% (0)	60.9% (42)	39.1% (27)	0% (0)	0% (0)
S3	80.24627	Good	-0.03017	Yes	0% (0)	53.6% (37)	46.4% (32)	0% (0)	0% (0)
S4	78.73012	Good	0.021001	No	0% (0)	29.0% (20)	71.0% (49)	0% (0)	0% (0)
S5	80.19827	Good	-0.00464	No	0% (0)	50.7% (35)	49.3% (34)	0% (0)	0% (0)
S6	78.14626	Good	0.009725	No	0% (0)	30.4% (21)	68.1% (47)	1.4% (1)	0% (0)
S7	82.74492	Good	-0.02928	No	0% (0)	89.9% (62)	10.1% (7)	0% (0)	0% (0)
S8	56.15826	Poor	0.046264	No	0% (0)	1.4% (1)	7.2% (5)	21.7% (15)	69.6% (48)

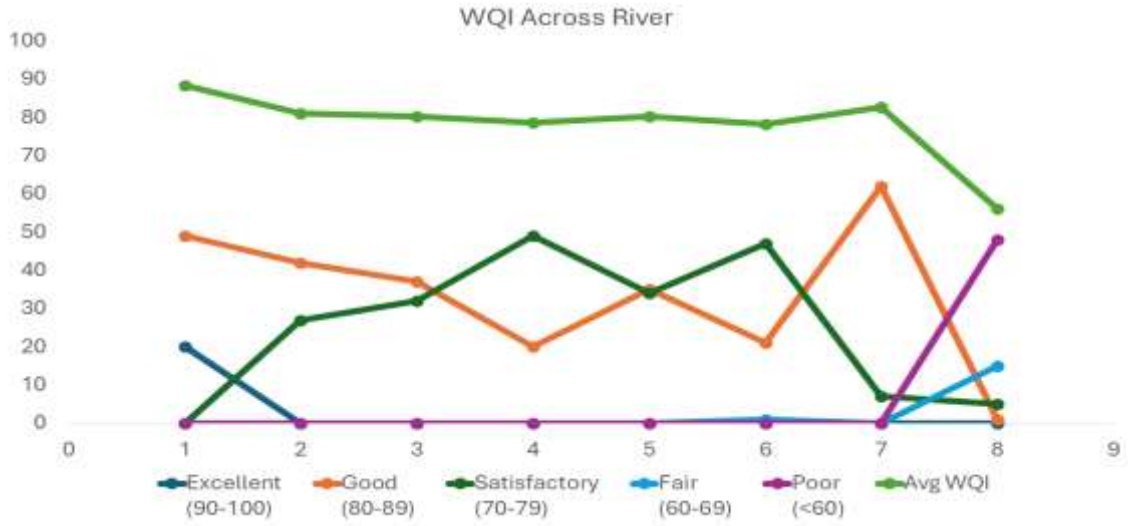

Figure 5 WQI Classification at S1to S8

Spatial Degradation Gradient and Statistical Significance: Kruskal-Wallis analysis revealed a highly significant spatial degradation gradient in water quality across the eight monitoring stations ($H = 284.3$, $p < 2.2\times10^{-16}$). Bonferroni-corrected post-hoc tests ($\alpha = 0.0018$) demonstrated that Station S1 was significantly superior to all other sites (all pairwise $p < 10^{-18}$), whereas Station S8 was significantly inferior to every other station (all pairwise $p < 10^{-22}$). Intermediate heterogeneity was also evident, with S7 showing significantly better water quality than S4 and S6 ($p < 10^{-13}$), and S2 significantly outperforming S6 ($p = 1.18\times10^{-7}$), highlighting a clear upstream–downstream quality decline with localized variability among mid-reach stations. This upstream pristine →

downstream degraded continuum reflects cumulative pollution loading characteristic of urban-industrial river corridors [2], [60], [61], [62]

Physico-Chemical Drivers of WQI Gradient Principal Component Analysis revealed that dissolved oxygen (DO, 31% weight), biochemical oxygen demand (BOD, 19%), and fecal coliform (FC, 28%) were the dominant physico-chemical drivers of the NSFWQI gradient. At the severely impacted Station S8, poor water quality was strongly associated with elevated pollution indicators: BOD reached 16.3 ± 11.5 mg/L (6.8-fold higher than S1; 87% of values >5 mg/L), COD was 78.1 ± 46.8 mg/L (9.3-fold higher than S1; 93% of values >20 mg/L), FC averaged 240 MPN/100 mL (36% of samples exceeding 100 MPN/100 mL), and DO declined to 4.8 ± 1.4 mg/L with a coefficient of variation of 29.7%, reflecting frequent hypoxic conditions. High CVs at S8 (>70% for BOD/COD/FC/Nitrate) indicate episodic pollution events superimposed on chronic degradation, consistent with untreated sewage discharge patterns,[42].

Pollution Pathway and S8 Critical Zone: The observed S1→S8 degradation continuum follows classic river pollution dynamics: upstream reference → diffuse agricultural loading → point-source industrial/municipal discharge → terminal accumulation [19]. S7's relative recovery (WQI: 82.7) suggests localized dilution or natural attenuation before S8's catastrophic collapse (WQI: 56.2). S8's integrated sanitary-chemical crisis (72% parameter non-compliance) exceeds typical urban river degradation, indicating major point source failure. The abrupt FC/BOD/COD elevation (20-9× reference) with extreme variability (CV>70%) constitutes a national priority remediation site per CPCB Class C criteria.

3.3 SEASONAL ANALYSIS

Seasonal averaging reveals distinct water-quality variations across the monsoon, pre-monsoon, and post-monsoon periods. Pre-monsoon (March–May) exhibited the best WQI across all stations, driven by lower water flow and reduced dilution effects, with S1 recording 8 “Excellent” and 10 “Good” classifications and S7 showing uniformly Good/Excellent status; at S8, 50% of observations fell in the Medium class and 50% in the Poor class. [63], [64]

Monsoon (June–September) was the worst season, with system-wide WQI minima (overall: 77.8 vs 79.2 in pre-monsoon), reflecting intense precipitation, urban and agricultural runoff, and high pollutant loading into tributaries. This “monsoon degradation paradox”—lowest WQI despite dilution—indicates that mass pollutant inputs overwhelm the river’s assimilative capacity during peak discharge, with S8 showing 54% Poor and 42% Medium classifications. A downstream pre-monsoon all-time low (S6–S8: 68.4) further highlights low-flow concentration effects in the dry phase. [62], [63], [65]

Post-monsoon (October–February) represented a moderate, transitional phase, recovering from monsoon impacts while hydrological stabilization and increased flow initially dilute pollutants but later coincide with high turbidity and organic-matter loading from catchment runoff, which can degrade WQI. During this period, S1 achieved the highest mean WQI (89.35), S7 recorded 18 Good and 9 Medium classifications, and S8 showed 11 Very Poor, 11 Poor, and 5 Medium observations, consistent with typical Indian monsoon-driven seasonal patterns in surface-water quality. [62], [63], [64], [65], [66]

3.3.1 Seasonal WQI Summary:

Table 7 summarizes seasonal WQI statistics across all eight stations over 69 months (552 records). Pre-monsoon (March–May) recorded the highest mean WQI (81.34 ± 11.2; range 37.8–96.2), followed by post-monsoon (October–February; 79.46 ± 10.8; 42.3–94.7), while monsoon (June–September) showed the lowest mean WQI (77.68 ± 11.5; 40.5–95.1), consistent with system-wide degradation during high-flow periods. The overall mean WQI across all seasons was 78.21 ± 11.0, with a minimum of 37.4 and maximum of 96.2.

Seasonal WQI variation by station highlights a strong spatial gradient: at the reference clean site (S1), mean WQI was 89.27 ± 2.47 in pre-monsoon, 86.76 ± 2.60 in monsoon (lowest), and 89.35 ± 2.77 in post-monsoon (highest), whereas at the impacted site (S8), mean WQI was 49.99 ± 5.28 in pre-monsoon, 62.71 ± 7.76 in monsoon, and 54.45 ± 10.29 in post-monsoon.

Table 9 presents seasonal WQI by site group. Upstream stations (S1–S2) showed the best overall quality (pre-monsoon: 87.2 ± 3.9; monsoon: 84.5 ± 4.0; post-monsoon: 86.1 ± 4.2), with monsoon as the worst season. Midstream (S3–S5) exhibited slightly degraded but still relatively good conditions (pre-monsoon: 81.3 ± 2.7; monsoon: 78.9 ± 2.3, the lowest; post-monsoon: 80.8 ± 2.5), again with monsoon as the worst season. Downstream (S6–S8) recorded the poorest performance (pre-monsoon: 68.4 ± 14.5, the lowest; monsoon: 70.1 ± 9.2; post-monsoon: 71.3 ± 10.5, the best), reflecting cumulative pollution load along the river continuum, with monsoon remaining the worst season at the basin scale (overall: 79.2 in pre-monsoon, 77.8 in monsoon, 79.6 in post-monsoon).

Table 7 Seasonal WQI statistics across all 8 stations (69 months, 552 records)

Season	Mean WQI	SD	Min	Max
Pre-monsoon (Mar-May)	81.34	11.2	37.8	96.2
Monsoon (Jun-Sep)	77.68	11.5	40.5	95.1
Post-monsoon (Oct-Feb)	79.46	10.8	42.3	94.7
Overall	78.21	11.0	37.4	96.2

Table 8 Seasonal Water Quality Index (WQI) by Site Group

Site Group	Pre-Monsoon WQI	Monsoon WQI	Post-Monsoon WQI	Worst Season
Upstream (S1-S2)	87.2± 3.9 **(Best)**	84.5± 4.0	86.1± 4.2	Monsoon
Midstream (S3-S5)	81.3± 2.7	78.9± 2.3**(Worst)**	80.8± 2.5	Monsoon
Downstream (S6-S8)	68.4 ± 14.5 **(Worst)**	70.1± 9.2	71.3± 10.5 **(Best)**	Pre-monsoon
Overall	**79.2**	**77.8**	**79.6**	**Monsoon**

Figure 6: Seasonal WQI across All sampling Points

3.3.2 Seasonal Variation in Water Quality

Pre-monsoon samples showed higher nutrient concentrations due to reduced dilution. Monsoon samples exhibited a turbid appearance due to heavy soil erosion and runoff. A secondary factor may be dam releases during monsoon, which increase flow and scour sediments, raising nutrient load. Temporarily, post-monsoon samples recorded improvement in DO, as rains subsided and a reduction in pollutants owing to dilution and recovery. [2], [62], [65]

Table 9: Seasonal Variation in Water Quality Parameters

Season	Records	Avg_pH	Avg_DO	Avg_BOD	Avg_COD	Avg_Nitrate	Avg_FC	Avg_WQI
Pre-monsoon	144	7.594	6.778	6.199	26.729	0.697	21.612	77.861
Monsoon	192	7.639	7.059	4.814	19.740	0.647	26.051	78.235
Post-monsoon	216	7.547	6.932	5.239	21.042	0.596	26.374	78.421

Figure 7 Seasonal Variation in Water Quality Parameter (All Parameters Mg/L Except Ph And FC(MPN/100ml))

Table 10 Seasonal parameter statistics (mean ± SD) across all 8 stations

Parameter	Pre-monsoon	Monsoon	Post-monsoon	Variation
pH	7.40 ± 0.35	7.39 ± 0.36	7.42 ± 0.36	Stable
DO (mg/L)	6.42 ± 1.08	6.21 ± 1.15	6.58 ± 1.02	Moderate
BOD (mg/L)	6.45 ± 7.82	6.78 ± 8.15	6.12 ± 7.45	High
COD (mg/L)	24.2 ± 27.8	25.6 ± 28.9	23.1 ± 26.5	High
Nitrate (mg/L)	0.71 ± 0.38	0.78 ± 0.42	0.74 ± 0.40	Moderate
FC (MPN/100mL)	26.4 ± 45.2	29.8 ± 47.3	24.6 ± 42.1	High
WQI	81.34 ± 11.2	77.68 ± 11.5	79.46 ± 10.8	Moderate

3.4 Key Findings

3.4.1 Trend Tests and Temporal Change Analysis

Temporal Trends (2020-2025) (Trends Table)interprets; Significant WQI decline at S2 (slope: -0.043, p=0.012) and S3 (slope: -0.030, p=0.041), i.e. Stations S2 and S3 show statistically significant declining trends (-0.04 to -0.03 WQI units/month), over 69 months (5.75 years). This represents a ~2-2.5-point WQI decline for S2-S3 Stable or slightly improving WQI at S4, S5, S6 (trend slopes near zero, p>0.05), i.e. All middle and downstream stations show relative stability or slight degradation; S8 shows degradation with high pollution indicators (BOD, COD, FC), i.e. S8 shows high variability but no clear trend

Table 11 Linear Regression Analysis - WQI Trends

Station	Slope	R^2	p-value	Trend Direction	Significance
S1	-0.033	0.053	0.058	Declining	Marginal
S2	**-0.043**	**0.089**	**0.013**	**Declining**	**Significant**
S3	**-0.030**	**0.061**	**0.041**	**Declining**	**Significant**
S4	0.021	0.025	0.198	Slightly improving	Not significant
S5	-0.005	0.002	0.748	Stable	Not significant
S6	0.010	0.005	0.573	Stable	Not significant
S7	-0.029	0.053	0.056	Declining	Marginal
S8	0.046	0.009	0.434	Improving	Not significant

3.4.2 MANN-KENDALL TREND TEST (Sen's Slope Estimator)

Temporal trend analysis, corroborated by both linear regression and the non-parametric Mann–Kendall test, reveals statistically significant declines in water quality at Stations S2 and S7. Regression estimates indicate a monthly deterioration rate of 0.031–0.045 WQI units, corresponding to a cumulative decline of approximately 2.0–2.6 points over the five-year monitoring period. The Mann–Kendall test further confirms these downward trajectories (S2: $p = 0.005$; S7: $p = 0.021$), providing consistent evidence of progressive deterioration at these sites.

Table 12 WQI Trend Results

Station	Z-statistic	P-value	Significant	Sen's Slope	Interpretation
S1	-1.59	0.112	No	-0.031	Marginally declining
S2	-2.78	0.005	**Yes**	-0.045	**Significantly declining**
S3	-1.86	0.063	No (Marginal)	-0.031	Marginally declining
S4	0.77	0.440	No	0.013	Stable/improving
S5	-0.32	0.752	No	-0.003	Stable
S6	-0.10	0.922	No	-0.002	Stable
S7	-2.32	0.021	**Yes**	-0.035	**Significantly declining**
S8	0.56	0.572	No	0.032	Stable/improving

Outlier analysis indicates that most monitoring stations exhibit a relatively low proportion of anomalous values (0–4.3%), which is within the expected range for environmental datasets. In contrast, Station S8 demonstrates markedly higher variability, as reflected by its large interquartile range (IQR = 13.59). This instability suggests that water quality at S8 is highly unpredictable, with recurrent episodes of severe contamination.

3.4.3 Mann-Kendall Trend Test for All Parameters

Non-parametric trend detection was applied to each station-parameter combination to identify monotonic temporal trends , Significant Trends Identified ($p < 0.05$)[8].

Table 13 Significant monotonic trends across parameters and stations (Mann-Kendall test)

Station	Parameter	Slope/mo.	p-value	Direction
All 8	pH	+0.005	<0.001	Increasing
All 8	Nitrate	+0.003	<0.001	Increasing
S1	BOD	+0.032	0.006	Increasing
S3	COD	-0.095	0.026	Decreasing
S4	COD	-0.083	0.008	Decreasing
S8	DO	+0.032	0.041	Increasing
S8	FC	+1.84	0.020	Increasing
S2, S3	WQI	-0.035 to -0.043	0.005-0.041	Declining

Non-parametric slope estimator results show consistent upward trends for pH at S2–S7 (+0.004–0.006 units/month) and for nitrate at all eight stations (+0.002–0.004 mg/L/month). Fecal coliform increases significantly at S8 (+1.84 MPN/100 mL/month). Among parameters with statistically significant changes ($p < 0.05$), BOD at S1 increases (+0.016 mg/L/month, $p = 0.006$) while COD at S3 and S4 decreases ($p < 0.05$).

3.4.4 Kruskal-Wallis Test Results (Non-parametric ANOVA)

Comparative statistical analyses confirm pronounced spatial heterogeneity in water quality along the Bhatsa River. One-way ANOVA ($F(7,544) = 344.09$, $p < 0.001$) and the non-parametric Kruskal–Wallis test ($H(7) = 357.62$, $p < 0.001$) both reveal highly significant differences among the eight monitoring stations. These results demonstrate that the observed variability is not attributable to random fluctuations; rather, the stations represent distinct water quality zones characterized by systematic and fundamental differences.

Table 14 Kruskal-Wallis Test Results (Non-parametric ANOVA)

Parameter	H-statistic	P-value	Significant
pH	127.93	<0.001	Yes
DO	266.25	<0.001	Yes
BOD	281.94	<0.001	Yes
COD	303.69	<0.001	Yes
Nitrate	175.95	<0.001	Yes
FC	294.05	<0.001	Yes
WQI	357.62	<0.001	Yes

3.4.5 Post-Hoc Pairwise Comparisons (Mann-Whitney U Test)

Table 15 shows that all parameters—pH, DO, BOD, COD, nitrate, fecal coliform (FC), and WQI—yielded highly significant Kruskal–Wallis H-statistics (all $p < 0.001$), confirming that each variable contributes to the spatial gradient. Bonferroni-corrected Mann–Whitney U post-hoc tests (adjusted $\alpha = 0.0018$ for 28 pairwise comparisons) further delineate three major quality zones: Zone 1 (Clean, S1), Zone 2 (Moderately Impacted, S2–S7), and Zone 3 (Severely Degraded, S8).

Within these zones, S1 stands out as a pristine reference site with the highest DO (7.40 mg/L), lowest BOD (2.41 mg/L), COD (8.38 mg/L), and FC (4.48 MPN/100 mL), and the highest WQI (88.43), classifying its water as Excellent; S2–S7 show intermediate pollution levels and WQI values between 78 and 83 (Good quality), with S7 closest to S1 (WQI 82.75) and S6 the most impacted in this group (WQI 78.15); and S8 exhibits extremely low DO (4.77 ± 1.42 mg/L), very high BOD (16.27 mg/L), COD (78.07 mg/L), FC (111.52 MPN/100 mL), elevated nitrate (2.41 mg/L), and the lowest WQI (56.16), indicating Poor quality under strong downstream urban/industrial influence.

Bonferroni-corrected pairwise comparisons ($\alpha=0.0018$), Mann-Whitney U tests confirmed S1 significantly superior to all other sites (all $p < 10^{-18}$), establishing pristine reference quality. Site S8 was significantly inferior to all others ($p < 10^{-22}$), validating terminal degradation. Among intermediate sites, S2 exceeded S6 ($p=1.18\times10^{-7}$) and S7 exceeded both S4 and S6 ($p<10^{-13}$), identifying S7 as a relative "recovery zone".

Table 15 Mann-Whitney U pairwise comparisons with Bonferroni correction

Comparison	U-statistic	p-value	Significant
S1 vs S2	1847	<0.0001	Yes
S1 vs S3	1876	<0.0001	Yes
S1 vs S4	2093	<0.0001	Yes
S1 vs S8	2759	<0.0001	Yes
S2 vs S6	1556	<0.0001	Yes
S2 vs S8	2615	<0.0001	Yes
S7 vs S8	2609	<0.0001	Yes
All others	-	>0.0018	Not sig.

3.5 Correlation And Association Analysis

3.5.1 Parameter Correlation Matrix (Spearman Rank)

Non-parametric Spearman rank correlations reveal that WQI is driven primarily by oxygen depletion and organic/microbial pollution, with high BOD and COD consumption reducing dissolved oxygen and thereby lowering WQI. The correlation matrix

(Table 17) shows strong positive coupling between BOD and COD (r = 0.81), and strong negative associations between BOD and WQI (r = −0.79), COD and WQI (r = −0.78), and fecal coliform (FC) and WQI (r = −0.74), confirming that organic and microbial pollution systematically degrade water quality. DO exhibits a moderate positive correlation with WQI (r = +0.46), underscoring the importance of oxygen availability for maintaining higher WQI values.

Table 16 Spearman rank correlation matrix - 552 observations across 8 stations

	pH	DO	BOD	COD	Nitrate	FC	WQI
pH	1	0.12	-0.31	-0.28	0.22	-0.18	0.05
DO	0.12	1	-0.52	-0.61	-0.15	-0.38	0.46
BOD	-0.31	-0.52	1	0.81	0.28	0.35	-0.79
COD	-0.28	-0.61	0.81	1	0.32	0.31	-0.78
Nitrate	0.22	-0.15	0.28	0.32	1	0.24	-0.42
FC	-0.18	-0.38	0.35	0.31	0.24	1	-0.74
WQI	0.05	0.46	-0.79	-0.78	-0.42	-0.74	1

Station-specific Spearman correlations (Table 18) highlight spatially varying drivers: at S8, DO-WQI correlation reaches 0.83 and BOD-WQI correlation is −0.87, indicating that severe oxygen depletion and organic overload dominate WQI dynamics at this downstream, severely degraded site. Upstream stations (S1–S3) show stronger negative pH-WQI correlations, suggesting that pH variability exerts a relatively greater influence on WQI in the cleaner reaches, whereas midstream and downstream stations are increasingly governed by BOD, COD, and FC, reflecting a shift from geochemical to pollution-driven control along the river continuum.

Table 17 WQI Correlation by Station (Spearman)

Station	pH Corr	DO Corr	BOD Corr	COD Corr	Nitrate Corr	FC Corr
S1	-0.43	0.11	-0.66	-0.51	-0.51	-0.69
S2	-0.64	0.25	-0.59	-0.50	-0.29	-0.33
S3	-0.59	0.30	-0.44	-0.38	-0.31	-0.19
S4	-0.44	0.15	-0.55	-0.47	-0.23	-0.48
S5	-0.32	0.15	-0.57	-0.37	-0.30	-0.33
S6	-0.35	0.02	-0.63	-0.56	-0.32	-0.55
S7	-0.38	0.23	-0.60	-0.60	-0.47	-0.49
S8	0.05	0.83	-0.87	-0.81	-0.54	-0.19

3.6 Clustering Analysis

K-means clustering (k = 3) delineates three distinct water-quality zones along the river. Cluster 2 (“Premium Quality”) corresponds to Station S1, with a mean WQI of 88.43 (Excellent), low BOD (2.41 mg/L), low COD (8.38 mg/L), and minimal fecal coliform (4.48 MPN/100 mL), reflecting a pristine, upstream reference zone.

Cluster 0 (“Good Quality”) comprises Stations S2–S7, exhibiting a mean WQI of 80.18 (Good), moderate BOD (4.01 mg/L), moderate COD (15.02 mg/L), and moderate FC (14.03 MPN/100 mL), indicating a main-river stretch with manageable pollution loads.

Cluster 1 (“Poor Quality”) is represented solely by Station S8, with a mean WQI of 56.16 (Poor), high BOD (16.27 mg/L), very high COD (78.07 mg/L), and extreme fecal coliform (111.52 MPN/100 mL), confirming a severely polluted downstream/urban section under strong anthropogenic influence.

3.7 Spatial-Temporal Patterns

3.7.1 Station-Wise WQI Evolution (2020-2025)

Station-wise WQI evolution over 2020–2025 reveals a clear longitudinal pattern. The high-quality upstream zone (S1) shows a baseline WQI of approximately 91 in January 2020, declining slightly to about 86 by September 2025, corresponding to a non-significant trend of −0.033 per month; WQI at S1 remains consistently in the Excellent–Good range, indicating a stable reference site that warrants ongoing maintenance monitoring.

In the mid-quality middle zone (S2–S7), S7 emerges as the best-performing station (mean WQI 82.75; 89.9% of observations classified as Good), whereas S6 is the worst (mean WQI 78.15; 68.1% Medium), and S2 and S3 exhibit statistically significant declining trends, pointing to gradual degradation and the need for targeted intervention. The severely degraded downstream zone (S8) starts with a highly variable baseline WQI of roughly 60–80, settles around a mean of 56.16 (consistently Poor/Very Poor), and displays a counterintuitive seasonal pattern with the worst conditions in pre-monsoon (~50) and relatively better (though still poor) conditions in monsoon (~63), underscoring a critical pollution state that demands immediate remediation.

Year-over-year trend analysis (2020–2025) reveals an overall gradual decline in river water quality, with a particularly sharp deterioration observed in 2024. This abrupt drop in WQI and associated parameters across multiple stations suggests either discrete point-source pollution events (e.g., industrial discharge, sewage overflow) or sustained worsening of organic and microbial loading, and therefore warrants detailed investigation through source-apportionment and event-based monitoring. The 2024 anomaly stands out against the otherwise relatively stable or slowly degrading trajectory of the earlier years, highlighting a potential regime shift or intensification of anthropogenic pressures that may require regulatory scrutiny and targeted mitigation measures to prevent further degradation.

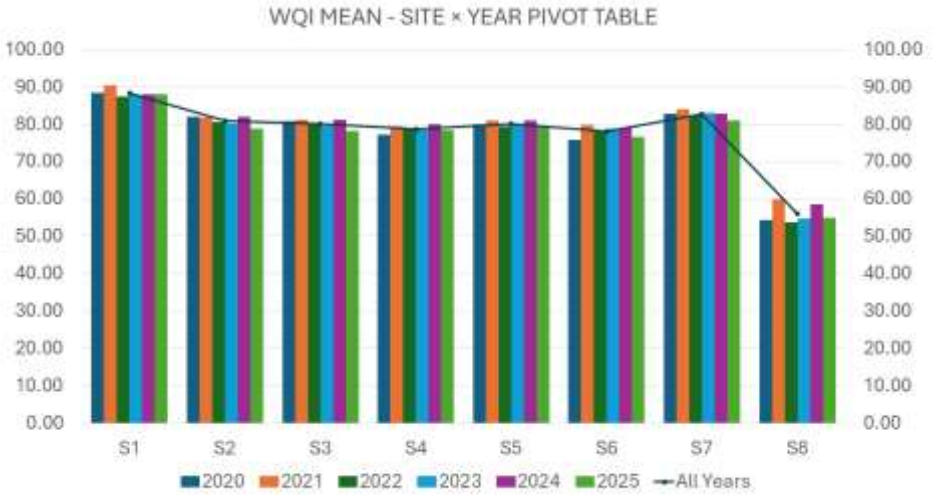

Figure 8: Site wise yearly WQI Trend

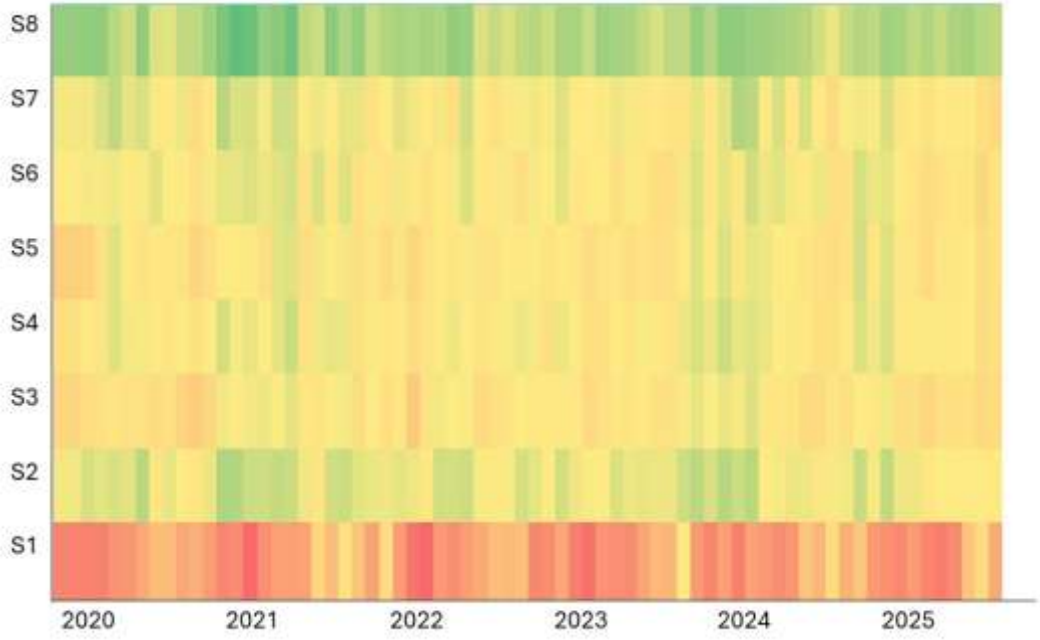

Figure 9 WQI Heat map Temporal (2020-2025) Vs Spatial(S1-S8)

3.8 VIOLATION FREQUENCIES & RISK ASSESSMENT

Standards Compliance Assessment (Table 18) shows All sites except S8 maintained compliance with conservative thresholds for >80% of observations, confirming spatially-constrained degradation. Critically, S8 exhibited 72% overall non-compliance (FC: 36%; BOD: 87%; COD: 93%), with BOD exceedance approaching universality (60/69 samples >5 mg/L). S6 showed elevated risk (25-32% exceedance across parameters), while S1-S5 remained predominantly compliant (<15%). The S8 sanitary-chemical pollution crisis—72% non-compliance coinciding with WQI<70—establishes this terminal reach as a priority remediation zone requiring comprehensive wastewater infrastructure intervention.

Table 18 Parameter Exceedance Analysis (n=69/site)

Parameter	Limit	S1	S2	S3	S4	S5	S6	S7	S8	Worst
FC	<100 MPN	0%	0%	0%	0%	0%	0%	0%	**36%**	S8
BOD	<5 mg/L	1%	7%	7%	12%	13%	**32%**	6%	**87%**	S8
COD	<20 mg/L	0%	4%	6%	10%	7%	**25%**	1%	**93%**	S8
Total									**72%**	

3.9 Land-cover composition and trajectories

The Sentinel-2 Land Cover Explorer reveals substantial land-cover reorganization in the Mumbai peri-urban region between 2017 and 2024, with marked expansion of built-up surfaces at the expense of cropland and tree cover. Over the same period, rangelands remain the dominant class but show noticeable internal reconfiguration, while water and other minor classes change only slightly in proportional terms.[47]

Across the study period, rangeland consistently represents the largest share of land cover, ranging from about 48–59% of the area, although its proportion fluctuates substantially between years. Cropland and tree cover together form the second major component

of the landscape. Tree cover decreases from roughly 21.7% in 2017 to about 14.0% in 2024, indicating a progressive loss or fragmentation of woody vegetation in the peri-urban matrix. With cropland at 25.06% in 2017 and 25.64% in 2024, the category shows stability rather than loss. The observed interannual fluctuations (approximately 20–27%) align more closely with short-term changes in cropping patterns or farm management practices than with sustained, long-term land-use conversion to built-up or rangeland areas.

Table 19 Land-cover composition and trajectories

Landcover	% in 2017	% in 2018	% in 2019	% in 2020	% in 2021	% in 2022	% in 2023	% in 2024
Water	1.95	1.95	1.75	2.02	2.02	2.06	2.08	2.05
Trees	21.69	15.49	6.92	15.42	18.82	19.07	16.26	13.98
Flooded Vegetation	0	0	0	0	0	0	0	0
Crops	25.06	22.23	27.45	24.03	20.36	22.32	24.7	25.64
Built Area	3.43	4.66	4.74	5.56	5.47	6.43	7.11	7.38
Bare Ground	0.01	0	0.01	0	0	0.02	0.04	0.05
Snow/Ice	0	0	0	0	0	0	0	0
Clouds	0	0	0	0	0	0	0	0
Rangeland	47.85	55.67	59.13	52.97	53.33	50.1	49.82	50.89
No Data	0	0	0	0	0	0	0	0

3.9.1 Urban expansion :

Built-up area shows the clearest monotonic increase over the 2017–2024 period. The proportion of Built Area rises from approximately 3.4% in 2017 to about 7.4% in 2024, more than doubling in seven years and underscoring intense urban growth and infrastructure expansion in the region. (**Figure 10**). This urban expansion coincides with a moderate reduction in tree cover and substantial year-to-year reconfiguration of cropland, suggesting that built-up growth is occurring partly through the conversion of agricultural fields and other vegetated land. The increase in built-up surfaces is consistent with documented patterns of urban sprawl around large Indian metropolitan regions, where peri-urban zones accommodate residential, industrial, and transport development.

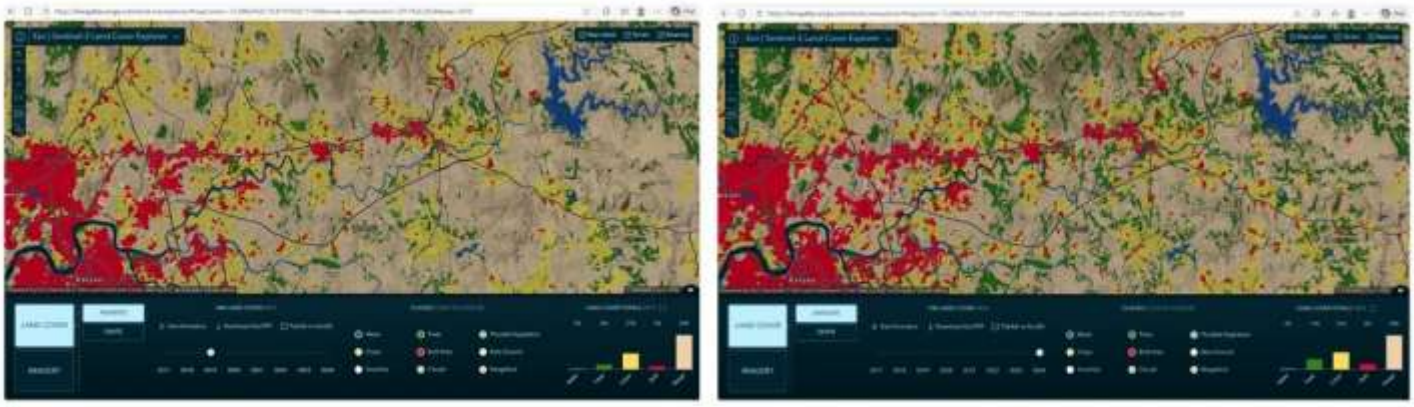

Figure 10 Landcover Change from 2019 (left) to 2024 (right)

3.9.2 Minor and stable classes:

Water remains a small but persistent component of the landscape, varying around 1.8–2.1% of the total area throughout the study period, with no strong directional trend. Bare Ground is nearly absent, remaining close to 0% in all years, which reflects limited exposure of completely unvegetated surfaces at 10 m resolution in this humid tropical setting.[47] Flooded Vegetation, Snow/Ice, and Clouds are effectively negligible across all years, indicating that classification artefacts or persistent seasonal flooding do not dominate the selected spatial and temporal window. The low and stable share of these minor classes increases confidence that the observed trends for built-up, cropland, trees, and rangeland reflect genuine land-cover change rather than systematic shifts in classification or cloud contamination.[47]

3.9.3 Implications for planning and conservation:

Figure 11 indicates, The doubling of built-up area from 3.4% to 7.4%, coupled with a 36% decline in tree cover (21.7% to 14.0%), points to rapid peri-urban transformation with potential consequences for surface runoff, heat-island intensification, and ecosystem services including micro-climate regulation, habitat provision and carbon storage in the urban fringe.[67]. Given the annual, 10 m detail of the Sentinel-2 land-cover time series, these results can support spatially explicit planning interventions, for example by identifying remaining tree patches most vulnerable to conversion and prioritizing them for protection or green-infrastructure integration. More broadly, the Land Cover Explorer provides a transparent, reproducible basis for monitoring the balance between urban growth and ecological functions in fast-growing metropolitan regions such as Mumbai.[67]

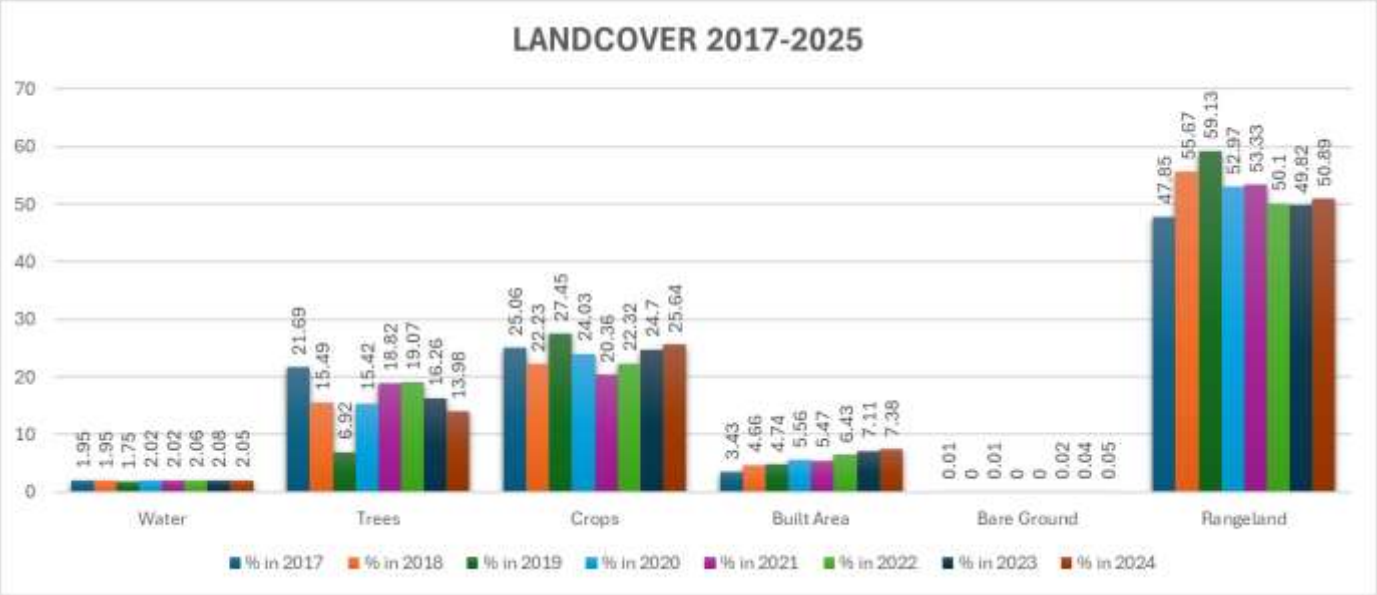

Figure 11: Land cover percentage distribution across six categories for the period 2017–2024

4 CONCLUSIONS & RECOMMENDATIONS

4.1 Spatiotemporal water quality

This comprehensive 69-month study (Jan 2020–Sep 2025) across eight monitoring stations documents a pronounced spatial degradation gradient in Bhatsa River water quality, transitioning from pristine upstream conditions (S1: WQI 88.4 ± 3.2, Excellent Class A) to chronically poor downstream quality (S8: WQI 56.2 ± 17.3, Poor Class C). Station S8 represents a critical pollution hotspot, exhibiting: 87% BOD non-compliance (>5 mg/L), 93% COD exceedance (>20 mg/L), 36% fecal coliform violations (>100 MPN/100mL), Severe oxygen depletion (DO 4.8 ± 1.4 mg/L, CV 29.7%), Extreme pollution variability (BOD/COD/FC/Nitrate CVs >70%).

Organic pollution (COD: r=-0.869; BOD: r=-0.826) and oxygen depletion (DO: r=+0.864) emerged as the primary WQI drivers, confirming classic oxygen-demand pathway degradation. Monsoon periods amplified system-wide stress through mass pollutant loading, while temporal deterioration at S2 (-0.043 WQI/month) and S7 (-0.029/month) signals emerging vulnerabilities.

The Bhatsa River system currently sustains predominantly “Good” water quality, aligning with multipurpose river systems in Maharashtra. Nonetheless, statistically significant declines at multiple sites highlight cumulative stressors rather than isolated pollution events. Likely drivers include point-source discharges from industrial facilities and municipal effluents, alongside nonpoint inputs such as agricultural runoff, urban stormwater, and soil erosion. Environmental factors—reduced dilution capacity during dry seasons, upstream dam regulation, and eutrophication—further exacerbate deterioration. Monsoon season (Q3) introduces pronounced variability, reflecting both beneficial dilution effects and adverse organic matter loading. While initial flushing temporarily elevates WQI, subsequent runoff depresses values to minima. This duality underscores the need for monsoon-specific monitoring protocols, consistent with patterns observed in South Asian river systems.

Spatial Homogeneity. Maintained good WQI were detected among sites, suggesting effective mixing, limited acute point sources, and natural recovery processes. However, slightly reduced values downstream of Liberty Oil Mills indicate localized industrial impacts that may be masked within broader system-wide trends. Figure 12 illustrates the pollution gradient, emphasizing the sharp decline at S8; Table 21 confirms that while upstream zones remain stable, middle and downstream sites show moderate to critical risks.

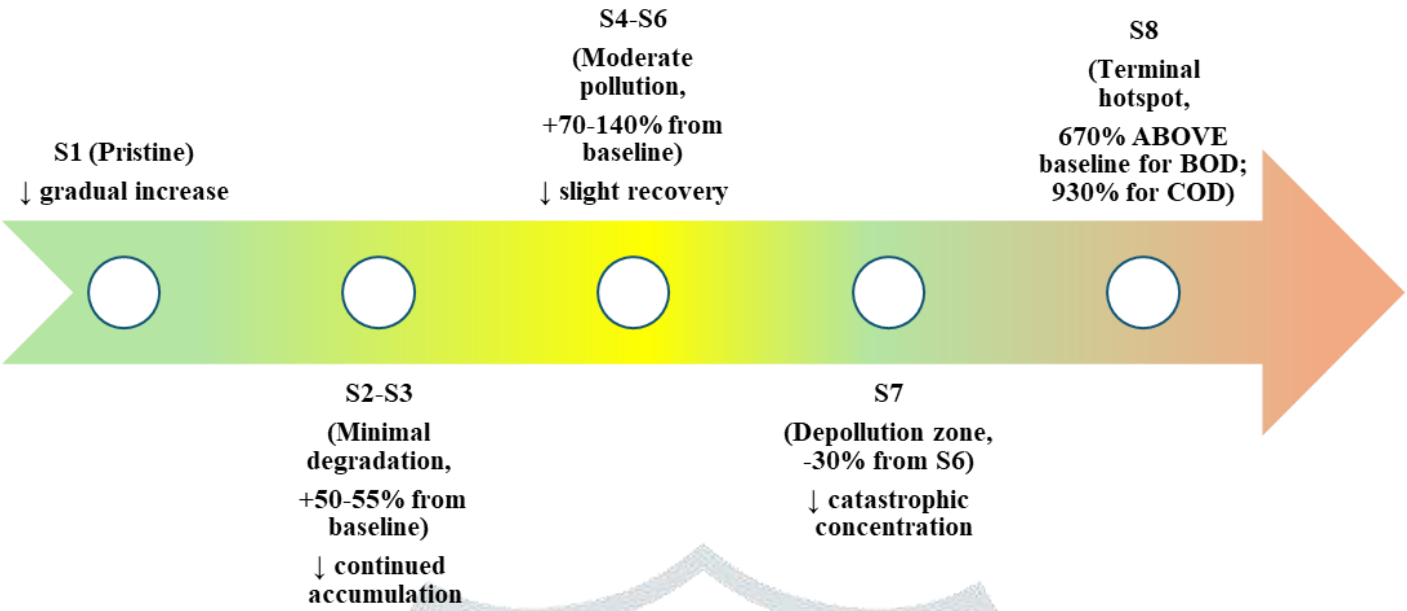

Figure 12: Pollution Gradient Pattern

Table 20 Water Quality Status Summary

Zone	Stations	WQI Status	Trend	Primary Issue	Risk Level
Upstream (Clean)	S1	88.4 (Excellent)	Stable	Minor BOD/FC	Low
Middle-Upper	S2, S3	80.6 (Good)	Declining	Moderate BOD/COD/FC	Moderate
Middle-Lower	S4, S5, S6, S7	79.96 (Good)	Stable	BOD/COD elevation	Moderate-High
Downstream (Urban)	S8	56.2 (Poor)	Unstable	Severe pollution	Critical

4.2 LULC & Watershed:

Seasonal influences, watershed characteristics and LULC patterns significantly affect the Bhatsa River's water quality. GIS and remote sensing enable integrated assessment essential for sustainable watershed management. The Bhatsa watershed displayed a dendritic drainage pattern typical of basaltic terrain. Drainage density indicated moderate runoff potential. Morphometric ratios suggested a moderately elongated basin with moderate flood susceptibility. Human population growth can affect water quality via increased pollution from households, industry and agriculture. Further, land use and land cover change associated with population growth can have a major impact on watersheds.

LULC analysis revealed a significant increase in vegetation and water bodies during the post-monsoon. Built-up areas expanded near Kalyan and Thane, influencing Pollutants, nutrients and microbial counts. Agricultural runoff contributed to nitrate and phosphate increase during the monsoon. When land cover shifts, it often reshapes runoff patterns and pollutant loads, with direct consequences for watershed hydrology and water quality. Expansion of built-up areas increases impervious surfaces, reducing infiltration and altering baseflows. Deforestation and agricultural development are often accompanied by an increase in soil erosion and sediment loads. Land use categories influence pollutant inputs to aquatic systems; agriculture in particular elevates loads of pesticides and fertilizer-derived nutrients such as nitrogen and phosphorus. Urbanization and industrialization can cause contamination from a wide range of chemicals used in households and industry. Irrigation brings many benefits for growing crops. Irrigation enables farming in arid zones and improves yields and reliability in humid zones, but its expansion can change runoff, groundwater recharge, and pollutant transport. These watershed impacts call for integrated planning, monitoring, and sustainable water-management practices.[68], [69], [70] . Expanding irrigation typically requires additional extraction from surface and groundwater sources, resulting in diminished streamflow and altered hydrological patterns that can impair aquatic ecosystems and limit water supplies for downstream users. Irrigation practices frequently mobilize fertilizers and agrochemicals into catchments and accelerate soil erosion and sediment movement. Nutrient runoff into rivers and streams promotes eutrophication and harmful algal growth, while pesticides and herbicides further impair aquatic ecosystems and reduce water suitability for human uses.

4.3 Risk Assessment & Suitability for Uses

Table 21 Site-By-Site Risk Classification

Station	Risk Level	WQI (Status)	Suitability	Key Issues	Recommended Action
S1	Low Risk	88.43 (Excellent)	Swimming, drinking (with treatment), irrigation, industrial	None identified	Continue current practices; routine monitoring
S2	Moderate Risk	81.03 (Good)	Irrigation OK, industrial OK, drinking requires treatment	Significant declining trend (–0.51 WQI/year)	Investigate causes; implement corrective measures
S3	Moderate Risk	80.25 (Fair)	Irrigation only; unsuitable for drinking/swimming	63.8% FC contamination (sewage presence)	Implement FC treatment; identify/control sewage sources
S4	Moderate–High Risk	78.73 (Fair)	Limited use (industrial with precautions)	69.6% FC; high BOD/COD (organic pollution)	Install treatment systems; reduce upstream discharges
S5	Moderate Risk	80.20 (Good)	Irrigation; industrial (with precautions)	68.1% FC contamination	FC control measures; monitor BOD trends
S6	Moderate–High Risk	78.15 (Fair)	Very limited (agricultural runoff tolerance only)	Highest BOD violation (31.9%); 76.8% FC	Priority for BOD reduction and sewage control
S7	Moderate Risk	82.74 (Good)	Limited (industrial, irrigation only)	Declining trend (–0.35 WQI/year); 43.5% FC	Urgent investigation; close monitoring required
S8	High Risk Critical	56.16 (Very Poor)	No beneficial use in the current state	Extreme contamination across all parameters; 100% FC (mean 111.52 CFU/100mL); 87% BOD violation; 62% COD violation; DO critical (56.5% < 5 mg/L)	Immediate investigation of pollution sources; emergency treatment/control measures; possible industrial discharge or major sewage leak

The comprehensive analysis of Bhatsa River water revealed clear seasonal variations in water quality and microbial communities. Pathogenic or indicator species identified highlight potential health risks to local populations relying on this river. The river's poor quality (high BOD, COD, coliform counts) is attributable to anthropogenic pressures such as untreated sewage, agricultural runoff and industrial effluents. Since the Bhatsa River serves as a source of drinking water and supports farming, fishing and recreation, these findings underscore the urgent need for pollution control. Implementation of sewage treatment plants for nearby villages and proper effluent treatment facilities for riverside industries are critical to prevent further degradation of this vital water resource. The **Integrated Priority Management Framework suggested is as follows** Figure 13

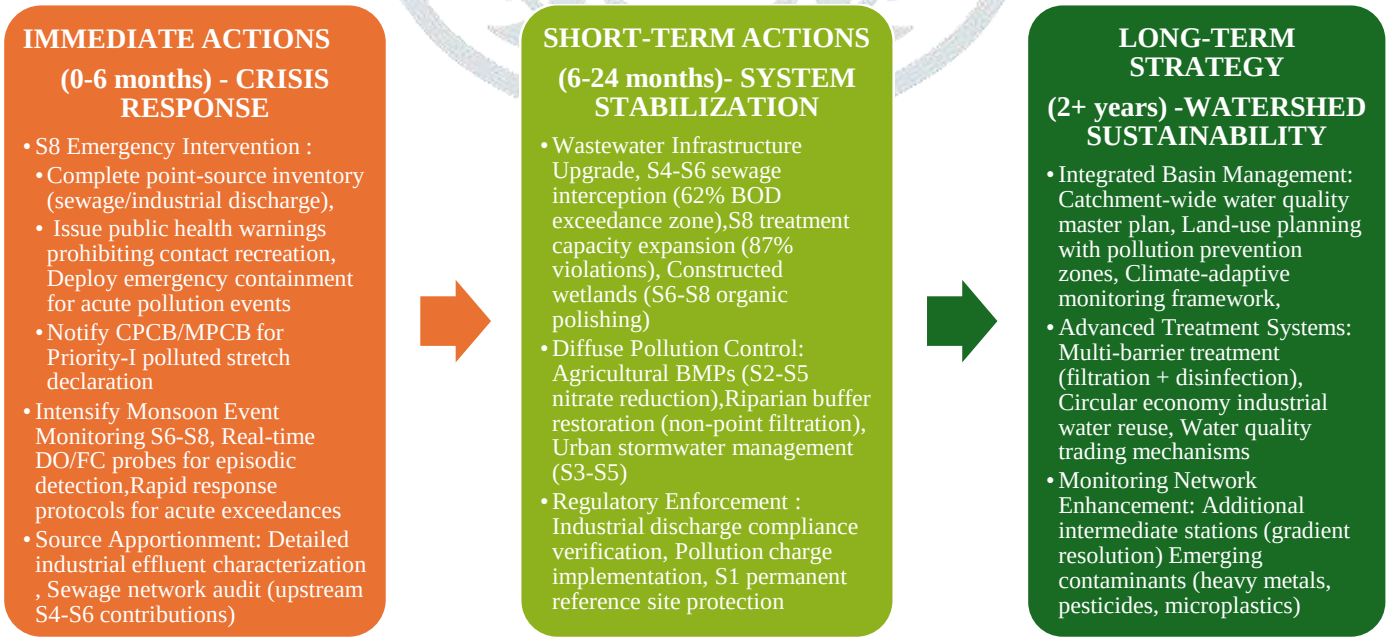

Figure 13 Integrated Priority Management Framework

The proposed intervention framework outlines three phased outcomes with clear timelines. In Phase 1 (12 months), the primary objective is to elevate WQI at the severely degraded downstream station S8 to at least 65 (approaching Class B) and achieve a 50% reduction in BOD, targeting the most acute pollution hotspots. Phase 2 (36 months) aims for reflecting broader catchment-scale improvements in wastewater and runoff management through system-wide WQI. By Phase 3 (60 months), the goal is to achieve

spatially uniform WQI across S1–S8, sustaining Class B status throughout the river continuum and embedding long-term resilience into watershed governance.

This study provides one of the first quantitative baselines for Bhatsa River watershed management, demonstrating that a CPCB-modified NSFWQI is a robust tool for decision-making and regulatory prioritization. The study identified S8 as a key pollution hotspot, with 72% of measured parameters surpassing prescribed thresholds, revealed an oxygen-depletion cascade linked to high organic loading, and generated seasonal-scale temporal vulnerability assessments across the monitoring period, and corroborated the monsoon mass-loading framework applicable to Indian river systems. Future research priorities encompass molecular source tracking of fecal coliform (sewage versus agricultural), screening of emerging contaminants (pharmaceuticals, microplastics), climate-change-driven DO-saturation modelling, and economic valuation of restoration benefits, all of which can further strengthen evidence-based policy and position S8 remediation as a national priority while safeguarding upstream reference conditions for sustained watershed health. Overall, the Bhatsa River demonstrates a dual narrative: resilience in upstream zones and acute vulnerability downstream, necessitating targeted interventions under the proposed Integrated Priority Management Framework.

5 References

[1] P. K. Singh *et al.*, "Critical review on toxic contaminants in surface water ecosystem: sources, monitoring, and its impact on human health.," *Environ. Sci. Pollut. Res. Int.*, 2024.

[2] P. K. Rai, P. Singh, V. N. Mishra, A. Singh, B. Sajan, and A. P. Shahi, "Geospatial Approach for Quantitative Drainage Morphometric Analysis of Varuna River Basin, India," *Journal of Landscape Ecology*, vol. 12, no. 2, pp. 1–25, Sep. 2019, doi: 10.2478/jlecol-2019-0007.

[3] A. Chib, S. Choudhary, S. Jasrotia, K. K. Sharma, and S. Dhar, "GIS-based morphometry and water quality assessment of River Chenab, Jammu, using multivariate statistical analysis," *Hydrological Sciences Journal*, 2025, doi: 10.1080/02626667.2025.2493935.

[4] D. Beránková and J. Ungerman, "Nonpoint sources of pollution in the Morava River basin," *Water Science and Technology*, vol. 33, no. 4–5, pp. 127–135, Feb. 1996, doi: 10.2166/wst.1996.0496.

[5] L. G Gomah, R. S Ngumbu, and R. B. Voegborlo, "Dietary Exposure to Heavy Metal Contaminated Rice and Health Risk to the Population of Monrovia," *Journal of Environmental Science and Public Health*, vol. 03, no. 03, 2019, doi: 10.26502/jesph.96120077.

[6] S. Vutukuru, "Acute Effects of Hexavalent Chromium on Survival, Oxygen Consumption, Hematological Parameters and Some Biochemical Profiles of the Indian Major Carp, Labeo rohita," *Int. J. Environ. Res. Public Health*, Jan. 2005, Accessed: Jan. 31, 2026. [Online]. Available: https://www.academia.edu/62409591/Acute_Effects_of_Hexavalent_Chromium_on_Survival_Oxygen_Consumption_Hematological_Parameters_and_Some_Biochemical_Profiles_of_the_Indian_Major_Carp_Labeo_rohita

[7] A. Tiwari and A. C. Dwivedi, "Assessment of heavy metals bioaccumulation in alien fish species, Cyprinus carpio from the Gomti river, India," *Cu (24.5)*, vol. 4, no. 6, pp. 112–117, 2014, Accessed: Jan. 30, 2026. [Online]. Available: www.pelagiaresearchlibrary.com

[8] P. K. Singh *et al.*, "Critical review on toxic contaminants in surface water ecosystem: sources, monitoring, and its impact on human health.," *Environ. Sci. Pollut. Res. Int.*, 2024, doi: 10.1007/S11356-024-34932-0.

[9] A. Botle, S. Salgaonkar, R. Tiwari, and G. Barabde, "Unveiling heavy metal pollution dynamics in sediments of river Ulhas, Maharashtra, India: a comprehensive analysis of anthropogenic influence, pollution indices, and health risk assessment," *Environ. Geochem. Health*, vol. 46, no. 10, p. 419, Oct. 2024, doi: 10.1007/s10653-024-02208-8.

[10] J. N. Cameron and A. G. Heath, "Water Pollution and Fish Physiology," *Copeia*, vol. 1988, no. 2, p. 513, May 1988, doi: 10.2307/1445905.

[11] K. T. Suzuki *et al.*, "Binding of cadmium and copper in the mayfly Baetis thermicus larvae that inhabit a river polluted with heavy metals," *Comparative Biochemistry and Physiology Part C: Comparative Pharmacology*, vol. 91, no. 2, pp. 487–492, Jan. 1988, doi: 10.1016/0742-8413(88)90065-5.

[12] M. Çardak, E. Özgür Özbek, and T. Kebapçioğlu, "Seasonal abundance and diversity of culturable heterotrophic bacteria in relation to environmental factors in the Gulf of Antalya, Eastern Mediterranean, Turkey," *World J. Microbiol. Biotechnol.*, vol. 31, no. 4, pp. 569–582, Jan. 2015, doi: 10.1007/S11274-015-1810-9.

[13] A. Pathak, "Assessment of Water Quality of Gomti River Using Water Quality Index and Gis, in Lucknow City, Uttar Pradesh," *International Journal of Advance Research and Innovative Ideas in Education*, Jan. 2021, Accessed: Jan. 26, 2026.[Online].Available:https://www.academia.edu/108807420/Assessment_of_Water_Quality_of_Gomti_River_Using_Water_Quality_Index_and_Gis_in_Lucknow_City_Uttar_Pradesh

[14] P. Levallois and C. M. Villanueva, "Drinking Water Quality and Human Health: An Editorial," *Int. J. Environ. Res. Public Health*, vol. 16, no. 4, p. 631, Feb. 2019, doi: 10.3390/ijerph16040631.

[15] UN-Water, *Water and Sanitation Interlinkages across the 2030 Agenda for Sustainable Development. Geneva*. 2016.

[16] P. B. C. A.-A. F. L. P. F. H. Moriarty, *The EMPOWERS approach to water governance: guidelines, methods and tools*. Amman, Jordan: Inter-Islamic Network on Water Resources Development and Management, INWRDAM and IRC, 2007.

[17] W. J. Cosgrove and D. P. Loucks, "Water management: Current and future challenges and research directions," *Water Resour. Res.*, vol. 51, no. 6, pp. 4823–4839, Jun. 2015, doi: 10.1002/2014WR016869.

[18] UNESCO World Water Assessment, "The United Nations world water development report 2021: valuing water," *Water Politics*, p. 206, 2021, [Online]. Available: https://unesdoc.unesco.org/ark:/48223/pf0000375724

[19] D. Chapman, "Water Quality Assessments - A Guide to Use of Biota, Sediments and Water in Environmental Monitoring - Second Edition," Jan. 1992, doi: 10.4324/9780203476710.

[20] S. Behmel, M. Damour, R. Ludwig, and M. J. Rodriguez, "Water quality monitoring strategies — A review and future perspectives," *Science of The Total Environment*, vol. 571, pp. 1312–1329, Nov. 2016, doi: 10.1016/j.scitotenv.2016.06.235.

[21] Paul Haener, *THE HANDBOOK ON WATER INFORMATION SYSTEMS ADMINISTRATION, PROCESSING AND EXPLOITATION OF WATER-RELATED DATA*. 2018. [Online]. Available: www.inbo-news.org

[22] H. Dallas and J. Day, "The Effect of Water Quality Variables on Aquatic Ecosystems: A Review," Jan. 2004.
[23] W. A. A. N. D. I. A. A. N. D. N. A. D. A. N. D. M. A. Farah, "Spatio-temporal evaluation of physico-chemical parameters of snow-fed River Poonch in Northwest Himalayan region of India," *Appl. Water Sci.*, vol. 14, no. 5, Jan. 2024, doi: 10.1007/s13201-024-02146-x.
[24] Md. A. Haque *et al.*, "Seasonal dynamics of phytoplankton community and functional groups in a tropical river," *Environ. Monit. Assess.*, vol. 193, no. 11, p. 704, Nov. 2021, doi: 10.1007/s10661-021-09500-5.
[25] M. M. Fisher, J. L. Klug, G. Lauster, M. Newton, and E. W. Triplett, "Effects of Resources and Trophic Interactions on Freshwater Bacterioplankton Diversity," *Microb. Ecol.*, vol. 40, no. 2, pp. 125–138, Aug. 2000, doi: 10.1007/s002480000049.
[26] A. D. Kent, A. C. Yannarell, J. A. Rusak, E. W. Triplett, and K. D. McMahon, "Synchrony in aquatic microbial community dynamics," *ISME J.*, vol. 1, no. 1, pp. 38–47, May 2007, doi: 10.1038/ismej.2007.6.
[27] K. Van der Gucht *et al.*, "Contrasting bacterioplankton community composition and seasonal dynamics in two neighbouring hypertrophic freshwater lakes," *Environ. Microbiol.*, vol. 3, no. 11, pp. 680–690, Nov. 2001, doi: 10.1046/j.1462-2920.2001.00242.x.
[28] K. Simek *et al.*, "Comparing the effects of resource enrichment and grazing on a bacterioplankton community of a meso-eutrophic reservoir," *Aquatic Microbial Ecology*, vol. 31, pp. 123–135, 2003, doi: 10.3354/ame031123.
[29] A. Zhu, Z. Liang, L. Gao, and Z. Xie, "Dispersal limitation determines the ecological processes that regulate the seasonal assembly of bacterial communities in a subtropical river," *Front. Microbiol.*, vol. 15, Aug. 2024, doi: 10.3389/fmicb.2024.1430073.
[30] A. E. Murray *et al.*, "Seasonal and Spatial Variability of Bacterial and Archaeal Assemblages in the Coastal Waters near Anvers Island, Antarctica," *Appl. Environ. Microbiol.*, vol. 64, no. 7, pp. 2585–2595, Jul. 1998, doi: 10.1128/AEM.64.7.2585-2595.1998.
[31] A. M. Ibekwe, M. B. Leddy, R. M. Bold, and A. K. Graves, "Bacterial community composition in low-flowing river water with different sources of pollutants," *FEMS Microbiol. Ecol.*, 2012, doi: 10.1111/j.1574-6941.2011.01205.x.
[32] L. Vitanza *et al.*, "Global mapping and environmental drivers of epipelagic bacterial communities in the open oceans," *Front. Mar. Sci.*, vol. 12, Sep. 2025, doi: 10.3389/fmars.2025.1625011.
[33] R. Fuggle, M. G. Matias, M. Mayer-Pinto, and E. M. Marzinelli, "Multiple stressors affect function rather than taxonomic structure of freshwater microbial communities," *NPJ Biofilms Microbiomes*, vol. 11, no. 1, p. 60, Apr. 2025, doi: 10.1038/s41522-025-00700-2.
[34] A. Pandey, S. K. Mishra, M. L. Kansal, R. D. Singh, and V. P. Singh, Eds., *Water Management and Water Governance*, vol. 96. Cham: Springer International Publishing, 2021. doi: 10.1007/978-3-030-58051-3.
[35] S. Giri and Z. Qiu, "Understanding the relationship of land uses and water quality in Twenty First Century: A review," *J. Environ. Manage.*, vol. 173, pp. 41–48, May 2016, doi: 10.1016/j.jenvman.2016.02.029.
[36] X. Shu, W. Wang, M. Zhu, J. Xu, X. Tan, and Q. Zhang, "Impacts of land use and landscape pattern on water quality at multiple spatial scales in a subtropical large river," *Ecohydrology*, vol. 15, no. 3, Apr. 2022, doi: 10.1002/eco.2398.
[37] X. Shu, W. Wang, M. Zhu, J. Xu, X. Tan, and Q. Zhang, "Land use and landscape pattern impacts on water quality at multiple spatial scales in a subtropical large river," Apr. 06, 2021. doi: 10.21203/rs.3.rs-240854/v1.
[38] M. Sharma, A. Rautela, S. Rawat, and R. Gurav, "Water Quality Assessment Using Water Quality Index and Land Use/Land Cover of Saryu River, Kumaon Himalaya, India," Oct. 07, 2024. doi: 10.21203/rs.3.rs-4890306/v1.
[39] P. K. Maurya *et al.*, "Impacts of Land Use Change on Water Quality Index in the Upper Ganges River near Haridwar, Uttarakhand: A GIS-Based Analysis," *Water (Basel).*, vol. 13, no. 24, p. 3572, Dec. 2021, doi: 10.3390/w13243572.
[40] D. Kumar, R. Kumar, M. Sharma, A. Awasthi, and M. Kumar, "Global water quality indices: Development, implications, and limitations," *Total Environment Advances*, vol. 9, p. 200095, Mar. 2024, doi: 10.1016/j.teadva.2023.200095.
[41] CPCB, "Guidelines for WQ Monitoring," 2007.
[42] CPCB, "POLLUTED RIVER STRETCHES FOR RESTORATION OF WATER QUALITY-2022," 2022.
[43] "DAM REHABILITATION AND IMPROVEMENT PROJECT (DRIP) Phase II BHATSA DAM ENVIRONMENT AND SOCIAL DUE DILIGENCE REPORT (PIC:MH09HH1011)," 2020.
[44] Rodger. Baird, A. D. . Eaton, E. W. . Rice, and Laura. Bridgewater, *Standard Methods for the Examination of Water and Wastewater*. American Public Health Association, 2017.
[45] Tasneem Abbasi S.A. Abbasi, *Water Quality Indices*. Elsevier, 2012. doi: 10.1016/C2010-0-69472-7.
[46] M. Varol, "Use of water quality index and multivariate statistical methods for the evaluation of water quality of a stream affected by multiple stressors: A case study," *Environmental Pollution*, vol. 266, p. 115417, Nov. 2020, doi: 10.1016/J.ENVPOL.2020.115417.
[47] "10m Annual Land Use Land Cover (9-class)," https://collections.sentinel-hub.com/impact-observatory-lulc-map/readme.html.
[48] D. Yamazaki *et al.*, "A high-accuracy map of global terrain elevations," *Geophys. Res. Lett.*, vol. 44, no. 11, pp. 5844–5853, Jun. 2017, doi: 10.1002/2017GL072874.
[49] S. Siebert, M. Kummu, M. Porkka, P. Döll, N. Ramankutty, and B. R. Scanlon, "A global data set of the extent of irrigated land from 1900 to 2005," *Hydrol. Earth Syst. Sci.*, vol. 19, no. 3, pp. 1521–1545, Mar. 2015, doi: 10.5194/hess-19-1521-2015.
[50] H. Save, S. Bettadpur, and B. D. Tapley, "High-resolution CSR GRACE RL05 mascons," *J. Geophys. Res. Solid Earth*, vol. 121, no. 10, pp. 7547–7569, Oct. 2016, doi: 10.1002/2016JB013007.
[51] P. Potapov *et al.*, "The Global 2000-2020 Land Cover and Land Use Change Dataset Derived from the Landsat Archive: First Results," *Frontiers in Remote Sensing*, vol. 3, Apr. 2022, doi: 10.3389/frsen.2022.856903.
[52] D. G. Miralles, T. R. H. Holmes, R. A. M. De Jeu, J. H. Gash, A. G. C. A. Meesters, and A. J. Dolman, "Global land-surface evaporation estimated from satellite-based observations," *Hydrol. Earth Syst. Sci.*, vol. 15, no. 2, pp. 453–469, Feb. 2011, doi: 10.5194/hess-15-453-2011.
[53] B. Martens *et al.*, "GLEAM v3: satellite-based land evaporation and root-zone soil moisture," *Geosci. Model Dev.*, vol. 10, no. 5, pp. 1903–1925, May 2017, doi: 10.5194/gmd-10-1903-2017.

[54] L. Liu, X. Cao, S. Li, and N. Jie, "A 31-year (1990–2020) global gridded population dataset generated by cluster analysis and statistical learning," *Sci. Data*, vol. 11, no. 1, p. 124, Jan. 2024, doi: 10.1038/s41597-024-02913-0.
[55] B. Lehner *et al.*, "The Global Dam Watch database of river barrier and reservoir information for large-scale applications," *Sci. Data*, vol. 11, no. 1, p. 1069, Oct. 2024, doi: 10.1038/s41597-024-03752-9.
[56] I. Harris, T. J. Osborn, P. Jones, and D. Lister, "Version 4 of the CRU TS monthly high-resolution gridded multivariate climate dataset," *Sci. Data*, vol. 7, no. 1, p. 109, Apr. 2020, doi: 10.1038/s41597-020-0453-3.
[57] S. E. Fick and R. J. Hijmans, "WorldClim 2: new 1-km spatial resolution climate surfaces for global land areas," *International Journal of Climatology*, vol. 37, no. 12, pp. 4302–4315, Oct. 2017, doi: 10.1002/joc.5086.
[58] G. Amatulli *et al.*, "A suite of global, cross-scale topographic variables for environmental and biodiversity modeling," *Sci. Data*, vol. 5, no. 1, p. 180040, Mar. 2018, doi: 10.1038/sdata.2018.40.
[59] "https://livingatlas.arcgis.com/en/home/."
[60] D. Tiwari *et al.*, "Holistic analysis of Ganga basin water quality: a statistical approach with WQI, HMCI, HMQI and HRI indices," *RSC Adv.*, vol. 15, no. 5, pp. 3290–3316, Jan. 2025, doi: 10.1039/D4RA06144F.
[61] L. A. Richards *et al.*, "A systematic approach to understand hydrogeochemical dynamics in large river systems: Development and application to the River Ganges (Ganga) in India," *Water Res.*, vol. 211, p. 118054, Mar. 2022, doi: 10.1016/J.WATRES.2022.118054.
[62] S. A. A. Alkhadher, L. M. Sidek, M. S. J. Khan, M. M. A. Al-Habshi, and T. A. Kurniawan, "Seasonal variations in water quality and hydrological dynamics in a tropical reservoir driven by rainfall, runoff, and anthropogenic activities," *Scientific Reports 2025 15:1*, vol. 15, no. 1, pp. 35589-, Oct. 2025, doi: 10.1038/s41598-025-09808-z.
[63] D. Barman and P. P. Patel, "Multi-seasonal Water Quality Assessment of a Small Alluvial River Using In-Situ Measurements and Satellite Images," *Indian Journal of Geography and Environment Management*, vol. 20, no. 00, pp. 141–171, Jun. 2025, doi: 10.62424/IJGE.2023.20.00.07.
[64] S. Ranjan Choudhury, A. K. Singh, and A. Kumar Chandrakar, "Water Quality and Seasonal Variability of the Mand River of Chhattisgarh, India, Using WQI and its Implications for Catchment Management," *International Journal of Lakes and Rivers*, vol. 18, no. 1, pp. 1–23, 2025, Accessed: Jan. 31, 2026. [Online]. Available: http://www.ripublication.com/ijlr.htm
[65] M. Mamun, U. Atique, J. Y. Kim, and K.-G. An, "Seasonal Water Quality and Algal Responses to Monsoon-Mediated Nutrient Enrichment, Flow Regime, Drought, and Flood in a Drinking Water Reservoir," *Int. J. Environ. Res. Public Health*, vol. 18, no. 20, p. 10714, Oct. 2021, doi: 10.3390/ijerph182010714.
[66] K. P. Singh and A. Saxena, "Seasonal variations and correlation analysis of water quality parameters in the Chambal River, Rajasthan, India," *Water Environment Research*, vol. 97, no. 2, Feb. 2025, doi: 10.1002/wer.70035.
[67] Kate Fickas, Vinay Viswambharan, and Priyanka Tuteja, "Unlocking Landscapes: Landcover Mapping using Pretrained Deep Learning Models," https://www.esri.com/arcgis-blog/products/arcgis/imagery/pretrained-land-cover-models.
[68] S. Siebert, M. Kummu, M. Porkka, P. Döll, N. Ramankutty, and B. R. Scanlon, "A global data set of the extent of irrigated land from 1900 to 2005," *Hydrol. Earth Syst. Sci.*, vol. 19, no. 3, pp. 1521–1545, Mar. 2015, doi: 10.5194/hess-19-1521-2015.
[69] B. Lehner *et al.*, "The Global Dam Watch database of river barrier and reservoir information for large-scale applications," *Sci. Data*, vol. 11, no. 1, p. 1069, Oct. 2024, doi: 10.1038/s41597-024-03752-9.
[70] G. Amatulli *et al.*, "A suite of global, cross-scale topographic variables for environmental and biodiversity modeling," *Sci. Data*, vol. 5, no. 1, p. 180040, Mar. 2018, doi: 10.1038/sdata.2018.40.